COMPARISON OF 3D ROTATIONAL ANGIOGRAPHY WITH DIGITAL SUBTRACTION ANGIOGRAPHY AND CORRELATION OF ANGIOARCHITECTURE WITH CLINICAL PRESENTATIONS IN CEREBRAL ARTERIOVENOUS MALFORMATIONS

THESIS

SUBMITTED IN PARTIAL FULFILLMENT FOR DEGREE OF

DM NEUROIMAGING AND INTERVENTIONAL NEURORADIOLOGY

(2017-2019)

OF

THE SREE CHITRA TIRUNAL INSTITUTE FOR MEDICAL SCIENCES AND TECHNOLOGY, TRIVANDRUM, INDIA

DR. SOMNATH PAN

DEPARTMENT OF IMAGING SCIENCES & INTERVENTIONAL RADIOLOGY, SREE CHITRA TIRUNAL INSTITUTE FOR MEDICAL SCIENCES AND TECHNOLOGY, TRIVANDRUM, INDIA

SREE CHITRA TIRUNAL INSTITUTE FOR MEDICAL SCIENCES AND TECHNOLOGY, TRIVANDRUM, INDIA

CERTIFICATE

This is to certify that the work incorporated in this thesis titled ***"Comparison of 3D Rotational Angiography with Digital Subtraction Angiography and Correlation of Angioarchitecture with Clinical Presentations in Cerebral Arteriovenous Malformations."*** *for the degree of* ***DM NEUROIMAGING AND INTERVENTIONAL NEURORADIOLOGY*** *has been carried out by* ***Dr. Somnath Pan*** *under our supervision and guidance. The work done in connection with this thesis has been carried out by the candidate himself and is genuine.*

Dr. Jayadevan ER	***Dr. Santhosh Kannath***	***Dr. Mathew Abraham***	***Dr. Ashalatha Radhakrishnan***
Additional Professor	***Associate Professor***	***Professor***	***Professor***
Principal Guide	***Co- Guide***	***Co-Guide***	***Co-Guide***

Dr Kesavadas C
Professor & HOD
Department of Imaging Sciences and Interventional Radiology,
SCTIMST, Thiruvananthapuram.

DECLARATION

I hereby declare that this thesis titled " Comparison of 3D Rotational Angiography with Digital Subtraction Angiography and Correlation of Angioarchitecture with Clinical Presentations in Cerebral Arteriovenous Malformation" has been prepared by me under the supervision and guidance of Dr.Jayadevan E R (Additional Professor), Dr.Santhosh K (Associate Professor) of Department of Imaging Sciences and Interventional Radiology, Dr. Mathew Abraham (Professor and HOD, Neurosurgery) and Dr. Ashalatha Radhakirshnan (Professor, Department of Neurology) Sree Chitra Institute for Medical Sciences and Technology, Trivandrum.

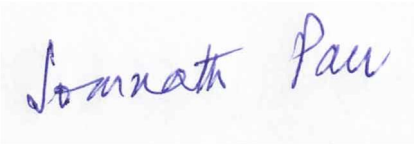

Date: 30 July 2019 *(Dr. Somnath Pan)*

Place: Thiruvananthapuram

ACKNOWLEDGEMENT

I am deeply indebted to my teachers & guides especially Dr. Jayadevan E R and Dr. Santhosh Kumar K of Department of Imaging Sciences and Interventional Radiology, for their constant unwavering support, insightful criticism and expert supervision throughout this study.

I am profoundly grateful to Dr.Kesavadas C, Dr. Bejoy Thomas, Dr. Mathew Abraham and Dr. Ashalatha Radhakrishnan for their support and guidance during this tenure.

I would specially like to acknowledge my gratitude to Dr.Gurpreet Singh for carrying out the statistical analysis of the study and for his valuable assistance at all times during the course of this study.

I would also like to extend my heartfelt gratitude to my family for being immensely supportive all through my endeavours.

Last but not least I am eternally grateful to all my patients & their relatives who have been very understanding and generous with their cooperation all through the study.

CONTENTS

INTRODUCTION

Brain arteriovenous malformations (AVM) are an intriguing disease entity involving the intracranial vasculature where arteries and veins are interconnected through a low resistance dysplastic nidus bypassing the normal intervening capillary network.[1]

There are several morphological aspects of AVM that need to be assessed prior to planning therapeutic approach and intervention. These include location, feeding arteries, draining veins, nidus and size of the lesion.[2] The presence of feeding artery, intranidal and perinidal aneurysms, venous pouches, venous dilatations, fistulas, venous stenosis and venous thrombosis are the other factors which necessitate therapy in brain arteriovenous malformations.[3,4] An ideal imaging modality should reliably reveal these parameters. Digital subtraction angiography (DSA) very reliably predicts the presence of these varied parameters. DSA is the standard imaging procedure for AVM. However, although it gives a good impression of the spatial relationships between the vessels, it is limited by overprojection of early draining veins on arterial feeders and nidus and cannot give a true three-dimensional (3D) view from every angle. The 3D rotational angiographic (RA) images have excellent resolution, and can be rotated in any direction to show the structures from any required angle, including views that would be impossible to obtain by radiographic projections alone. An improved understanding of the 3D vascular morphology helps to ensure optimum positioning of the image intensifier during the intervention for guideline positioning of catheters, coils, balloons and stents.[5] There are few studies comparing the utility of 3D RA in cerebral aneurysm.[6,7] Hochmuth A *et al.,* in their study have concluded that compared with DSA, 3D RA allows more exact

depiction of anatomic details that are important in planning surgery and interventional therapy for intracranial aneurysms and also RA depicted more aneurysms.[8] The current gold standard in imaging of brain AVM is superselective microcatheter angiography. We intended to study the effect of addition of 3D RA in better delineation of angioarchitecture of the lesions.

Cerebral AVM has varied clinical presentations. Broadly it can present because of haemorrhage and unbled lesions can manifest with seizure, headache, neurodeficit or vague neurologic symptoms. Also asymptomatic lesions are detected incidentally due to neuroimaging for inexplicit symptoms. Various angiographic features like deep venous drainage, deep location, infratentorial location, distal flow related & intranidal aneurysm, previous haemorrhage has been implicated as risk factors or predictors of haemorrhagic complications.[9] Few studies have attributed manifestation of seizure in AVM to angiographic features like cortical location of feeder, feeder by MCA, absence of aneurysm, varix/varices in venous drainage.[10] Other clinical manifestations like headache and neurodeficit in unbled AVM has not been studied in relation to specific angiomorphologic attribute. Combining the 2D DSA & 3D RA is expected to generate the best possible angiomorphology of AVM. We intend to analyse the angiographic predictors for clinical manifestations of haemorrhage, seizure, headache & neurodeficit; thereby prompting necessary therapeutic intervention.

AIMS AND OBJECTIVES

- To compare 3D RA & 2D DSA in the evaluation of angioarchitecture of AVM
- To propose angioarchitectural predictors for clinical presentations like haemorrhage, seizure, headache & neurodeficit in AVM

REVIEW OF LITERATURE

INTRODUCTION

Cerebral AVM is an intriguing vascular disease entity where a cerebral arteriovenous interconnection occurs through an intervening dysplastic nidus with absence of normal intervening capillary network in between the arterial tree and the venous drainage. The reported incidence of Brain AVM is 1.34/100,000-person years and the prevalence is 10 - 18/100,000. Brain AVM is the disease entity responsible for about 2% of haemorrhagic strokes.[11]

ETIOLOGY

The exact etiologic nature of cerebral arteriovenous malformations is still a question of debate with both congenital and acquired origins being attributed as the cause.

Initially brain AVM was regarded as congenital lesion representing inborn errors of embryonic vascular morphogenesis caused by a defect or malfunction of the embryonic capillary maturation process and resulting in the formation or persistence of arteriovenous shunts.[12]

But the relative paucity of in utero detection of Brain AVM on antenatal imaging is a deterrent to definite acceptance of the congenital nature of these lesions.

There is increasing evidence that the majority of brain AVMs, with the exception of aneurysmal malformations of the Galenic veins, develop postnatally and represent a complex endothelial cell dysfunction, triggered by still unknown factors. In favour of this hypothesis are immune-histochemical studies performed on surgically obtained

specimens of human brain AVMs which demonstrated, that the preproendothelin-1 gene is locally repressed in brain AVMs.[13] In addition, predominant expression of vascular endothelial growth factor in the subendothelial layer and in perivascular spaces of vessels composing brain AVM was demonstrated.[14]

Both primitive penetrating type and adult pattern functional or en-passage arteries and embryonic or adult pattern of veins have been described in the pathological studies of brain AVM.[15] Therefore, AVM has been thought of both as abnormalities of persistent primitive vascular plexus and also as proliferative capillaropathy.

AVM is a disease, present in nascent form at fetal stage, with acquired proliferative growth, becomes detectable or manifests later in life.

LOCATION OF BRAIN AVM

BAVMs are categorized based on vascular anatomic – topographic divisions into i) superficial (cortical) and ii) deep types. This was achieved with the routine application of MR imaging in the pretherapeutic evaluation of brain AVM.[16]

i) Cortical (superficial or convexity or pallial) AVM

This group is subcategorized into sulcal, gyral and mixed (sulcogyral) types.

Sulcal AVM: Sulcal AVMs are primarily located within a specific sulcus. Primary arterial supply is from terminal pial branches. The most superficial aspect is covered by the meninges; meningeal arterial supply to the superficial aspect is common.[17] Sulcal AVMs may be confined

to a sulcus or may extend into the depths of the sulcus, through underlying cortex into the subcortical white matter and even to the ventricular wall. The nidus of sulcal AVMs adapts to the geometric space of the sulcus and assumes a pyramidal or conical shape. Depending on their size and extension, sulcal AVMs are therefore further classified into three subtypes: (1) pure sulcal, (2) sulcal with subcortical extension and (3) sulcal with subcortical and ventricular extension.[18]

Gyral AVM: Gyral AVMs are covered by cortex and are typically spherical. The gyrus usually is enlarged and adjacent sulci are compressed. A large gyral AVM may extend into the subcortical white matter toward the ventricular wall. The arterial supply is primarily from non-terminal pial branches; meningeal supply typically is absent.[17]

Mixed sulcogyral AVM: Theses are large cerebral AVMs that combine both sulcal and gyral features, they typically involve gyri and sulci and extend into the subcortical white matter to the ventricular wall. Arterial supply includes terminal and non-terminal pial branches, basal perforating arteries and meningeal arteries.[17]

ii) Deep (central) brain AVM

They can be subdivided into subarachnoid, deep parenchymal, plexal, and mixed types.

Subarachnoid AVM: They are found in the basal cisterns and fissures, supplied by the subarachnoid portions of the choroidal and perforating arteries.[18]

Deep parenchymal AVM: These AVMs are located in the deep brain structures (basal ganglia, thalamus, hypothalamus, septum pellucidum, corpus callosum, limbic system, internal capsule, other deep white matter

tracts and nuclei). They are supplied by basal perforators, choroidal arteries, basal circumferential arteries, and medullary pial branches.[18]

Plexal AVM: They are intraventricular, supplied by the choroidal arteries in a direct fashion. Larger plexal AVMs in contact with the ventricular wall or adjacent periventricular parenchymal involvement receive additional supply from subependymal arteries.[18]

Mixed deep AVM: They are larger, combining subarachnoid, deep parenchymal, and plexal features. Venous drainage is predominately into the deep venous system; however, transmedullary cortical venous drainage also is seen.[17]

ANGIOARCHITECTURE OF CEREBRAL AVM

The term 'angioarchitecture' refers to the angiographically demonstrable vascular elements composing a brain AVM. It includes the feeding arteries, the nidus, the draining veins, any associated vascular anomalies and secondary changes induced by the high-flow of the AVM (high-flow angiopathy).

Arterial feeders:

AVM arterial feeders are classified based on anatomic, geometric, and hemodynamic criteria. The arterial feeders can undergo high-flow related changes such as vascular hypertrophy and development of feeding artery aneurysms.

A. Geometric classification:

The term 'geometric' refers to the angiographically demonstrable relationship between a feeding artery with the nidus and the supply of normal brain parenchyma.[18] Three types of supply are seen: terminal,

pseudoterminal, and indirect.[19,20]

i) Terminal (Direct type) feeding arteries end directly in the nidus without continuation towards normal brain distal to it.[19] The main trunk of a direct type feeding artery may terminate in the nidus either as a single artery (monoterminal type) or may divide into two or more branches (multiterminal type).

ii) *Pseudoterminal arterial feeder* appears to end in the nidus, but has a distal segment supplying normal parenchyma that is not angiographically visible because of high flow ("sump effect") into the nidus. Embolization performed through a pseudoterminal type of feeder carries a risk for an ischaemic complication.[19,20]

A wedged catheter position or spasm of the arterial feeder during superselective angiography can give rise to pseudoterminal feeder appearances.

iii) *Indirect types of feeder* refers to those primarily supply the normal brain with secondary participation into the supply of the AVM nidus. Two types of indirect supply of an AVM can be distinguished, i.e. en-passage (transit) feeders and retrograde collateral feeders.

En-passage or transit artery refers to an arterial trunk coursing close to the nidus of an AVM. It gives off one or several small and short branches to the nidus and its course distal to the nidus supplies normal brain parenchyma. [19,20]

Retrograde collateral feeding arteries belong to the arterial system distal to the AVM. Their antegrade flow distal to the AVM is compromised by the sump effect of the nidus. Reconstitution of flow is provided through compensatory recruitment of leptomeningeal collaterals. Therefore, flow

in the artery distal to the AVM is reversed. This phenomenon has been called ‘watershed transfer’.[20] With watershed transfer, angiogenesis can occur in response to chronic parenchymal ischemia.

B. Anatomical classification:

i) Pial feeding arteries supply the AVMs by extracortical (subpial), cortical, medullary, and/or corticomedullary branches. The feeding arteries to cerebral AVM are usually from the anterior or posterior intracranial circulation and arise depending upon the location of the AVM.

ii) *Perforating arteries* provide the main supply to the majority of deep brain AVMs.

iii) *Choroidal feeding arteries* (anterior, posterior medial and posterior lateral choroidal arteries) supply plexal AVMs in dominant way and deep brain AVMs with or without intraventricular extensions in a dominant or supplementary fashion.

iv) *Dural (meningeal) feeding arteries* supply the AVMs which are in contact with the dural-arachnoid-pial layers, and also some deep subarachnoid AVMs with direct contact to the tentorium. Usually they are direct and supplementary feeders.

Brain tissue ischaemia distal to the AVM may recruit meningeal arteries as collateral arteries. These dural arteries subsequently enlarge to supply AVM.[21] Subarachnoid haemorrhage may secondarily increase dural supply to an AVM.[22]

v) *Retrograde collateral feeding arteries* develop in association with watershed transfer and provide supplementary supply to the AVM as

detailed previously.

C. Haemodynamic classification

Feeding arteries may be characterized hemodynamically into dominant or supplementary according to the amount of flow. Most AVMs (82%) contain a combination of both types.[17] Some AVMs (13%) are supplied by multiple supplementary feeders, particularly observed with insular, some gyral and brain stem AVMs. A few AVMs (5%) are supplied exclusively by one or few dominant type feeding arteries, mainly seen with predominant fistulous AVMs.

Arterial high-flow angiopathy

'High-flow angiopathy' refers to the arteriovenous shunt induced secondary changes of arterial and venous circulation. The arterial high-flow angiopathy includes the following:

A. Arterial enlargement and variations

Development of extra-and intracranial dolichoectasia and loops are common with brain AVM. Arterial variations are reported to occur more frequently in brain AVM patients.[23]

B. Arterial stenoses

Brain AVM causes feeding artery or more proximal artery stenoses in up to 20% of cases. Such stenosis may be isolated or multifocal. Diffuse stenoses with a moyamoya appearance may be seen in younger patients.[20]

C. Brain AVM (BAVM) associated Aneurysms

Epidemiology

The reported prevalence of aneurysms associated with brain AVMs varies widely from 5.8% to 58%.[24-35] This variability probably arises from a number of factors, including: differing definitions, data collection methodology, varied imaging techniques, and inclusion criteria.

Reported multiplicity of BAVM-associated aneurysms is common. Almost half of the patients with BAVM associated-aneurysms will have more than one aneurysm.[28,29,36]

Classification

The Tew classification (Table 1) divides BAVM associated aneurysms into four groups based on their relationship to the feeding arteries and nidus.[37] This classification suggests potential mechanisms for aneurysm formation based on location. In addition, it has proven useful in attempts to relate aneurysm types to clinical behavior.[38]

Table 1. Tew classification of BAVM associated aneurysms.

Type I	Dysplastic or remote, not related to BAVM supply
Type II	Proximal, arising from the circle of Willis or origin of a vessel supplying the BAVM
Type III	Pedicular, arising from the midcourse of a feeding pedicle
Type IV	Intranidal, within the BAVM nidus

Alternately, these aneurysms can be distinguished into two types: (A. Valavanis and M.G. Yasargil)[18]

A. Flow-related aneurysms (those occurring on the arteries related haemodynamically to the supply of the AVM, 40 – 70% of all aneurysms)

    a. Proximal

    b. Distal-extranidal

    c. Distal-intranidal

B. Not flow-related aneurysms (those located on arteries not related haemodynamically to the supply of the AVM, 10 – 20% of all aneurysms)

Pathogenesis

Three major theories have addressed the association of BAVMs and aneurysms: coincidental occurrence, an underlying congenital vascular defect responsible for both lesions, and the flow-related (hyperdynamic) theory.

Most studies report a considerably higher frequency of aneurysms occurring in association with BAVMs. Therefore, theory of coincidental simple chance occurrence, is currently given little credence.[24-35]

To date, no underlying congenital defect has been identified to explain an association between aneurysms and BAVMs. A number of genes have been found to be differentially expressed in AVM feeding pedicles compared with normal cerebral arteries. This differential expression is likely a consequence of increased flow dynamics rather than

an underlying cause of the AVM-associated aneurysm.[39]

Flow phenomena provide a logical mechanism to explain BAVM-associated aneurysms. This theory, introduced by McKissock over 50 years ago, attributes the development of aneurysms to the hyperdynamic flow caused by AV shunting through the AVM.[40] Hyperdynamic flow increases shear stress on the vessel walls and this has been found to play a role in the formation, growth, and rupture of all types of arterial aneurysms.[41-43] Supportive facts for this theory includes the following observations. Aneurysms arise far more commonly on arterial feeders to the BAVM than on unrelated vessels. Aneurysms occur more often on arteries feeding larger, high-flow BAVMs than on arteries supplying smaller, low-flow BAVMs.[30,31,44] Also, BAVM-related aneurysms can decrease in size or disappear following treatment of the BAVM and correction of the high-flow state.[30]

Controversy surrounds the etiology of intranidal aneurysms. Most reports suggested these to be true aneurysms located in the most distal arterial branches. Others have suggested that some of these may represent early filling of dilated venous pouches or represent pseudoaneurysms arising as a result of hemorrhages.[45]

Clinical implications

The natural history of AVMs with associated aneurysms has been the subject of considerable controversy.

Some data suggest there are increased rates of both initial and recurrent hemorrhage when aneurysms are associated with BAVMs. In one series, patients with an BAVM-associated aneurysm had significantly higher annual hemorrhage risk of 7% at 5 years following diagnosis, than

the 1.7% rate for BAVMs without coexisting aneurysms.[26] In several series studying BAVMs accompanied by aneurysms presenting with hemorrhage, the aneurysm was considered to be the source of the hemorrhage in 50–80% of the cases.[31,34] Redekop *et al.,* found intranidal aneurysms were associated with a higher incidence of initial hemorrhage as well as with multiple episodes of recurrent bleeding.[30]

In contrast, other studies did not find initial BAVM hemorrhage to correlate with any type of aneurysm. [25,28]

Infratentorial BAVM-associated aneurysms may behave in an especially aggressive fashion. A study of 222 BAVMs identified five aneurysms associated with infratentorial BAVMs and 75% were responsible for intracranial hemorrhage.[32] Kaptain *et al.,* evaluated 27 cerebellar BAVMs, all of which were associated with aneurysms; 89% had findings of aneurysm rupture.[46] Khaw *et al.,* also reported a higher prevalence of aneurysms associated with infratentorial BAVMs; these were significantly more likely to present with intracranial hemorrhage than BAVMs without associated aneurysms.[47]

AVM Nidus

The nidus of an AVM represents the area of arteriovenous shunting, interposed between the distal segments of feeding arteries and emerging proximal segments of draining veins.[17]

Vascular composition of nidus

Angiographically, two main patterns (plexiform and fistulous categories) of arterivenous (AV) shunting can be distinguished depending upon the rate of flow and calibre of the AV shunt sizes.

In the plexiform type of nidus, one or several arterial feeders end in a vascular conglomerate of multiple AV microcommunications from which one or multiple venous channels emerge as draining veins.

In the mixed plexiform and fistulous type of nidus additional single or multiple feeding arteries end directly either in an end to end or in an end to side fashion along a draining vein or veins (fistulae).

General angiographic appearance of nidus

The AVM nidus is categorised as compact or diffuse / sparse depending upon the presence of intervening brain parenchyma within and the definition on the AVM boundaries (definitions and criteria elaborated in the discussion section).

Intranidal cavities

Superselective angiography may demonstrate intranidal vascular cavities.[20] They may be categorized as arterial aneurysm, arterial pseudoaneurysm, arterial loops, venous pseudoaneurysm and intranidal venous varix.

MRI is ideal for detecting intranidal non-vascular cavities. They may be normal or gliotic brain parenchyma or haemorrhagic cavities. Intranidal calcific foci are best depicted on CT scans.

Perinidal angiogenesis

Perinidal angiogenesis represents a secondary angiogenic response to chronic hypoperfusion or ischaemia induced by the AV shunt of the nidus. Morphologicallly it can be localized, moderate or even extensive, simulating a diffuse nidus (pseudo-diffuse nidus). Failure of recognition of perinidal angiogenesis may lead to overestimation of the true size of

the nidus.

Draining veins

On the venous side, the nidus can be drained by a single or multitude of veins. The drainage can be into deep venous system or to the superficial system, a characteristic which is primarily dependant on the location of the AVM. Cortical BAVMs typically drain through cortical veins into nearby dural sinuses. Those with subcortical or ventricular extension often have both superficial (cortical) and deep (subependymal) venous drainage. Central BAVMs usually drain into the deep venous system.

Unexpected venous drainage patterns, however, such as transcerebral cortical venous drainage of a deep BAVM or deep venous drainage of a cortical BAVM, may be seen approximately 30% of the time. These probably represent venous collaterals that developed after occlusion of the original venous drainage system.[20]

Haemodynamic types of draining veins: The draining veins may be classified into main and accessory types. Main draining veins are characterized angiographically by larger caliber and higher flow than accessory draining veins.

High-flow venous angiopathic changes result in ectasia, stenosis, the development of collateral venous circulation and competition between the venous drainage of the AVM and the normal brain.

Venous obstruction may be due to extramural, mural and intraluminal causes. Venous obstacles of extramural origin include mechanical compression of the dilated draining vein by rigid extracerebral structures such as the tentorial edge, the sphenoid ridge or

the falcotentorial junction and compression by pial arteries bridging over draining cortical veins. Venous obstacles of mural origin are focal stenosis of the wall of the draining vein occurring as an endothelial reaction and wall remodeling because of high flow. Venous obstructions of intraluminal origin are caused by spontaneous thrombosis of the venous lumen.

Irrespective of the cause, such obstructions increase the venous pressure proximally and induce collateral circulation to mitigate the venous hypertension. Depending on the location of the AVM with respect to the venous system, such collateral rerouting may occur by way of ipsilateral, contralateral or transcerebral veins.[20]

Insufficiently developed collateral venous drainage may result in venous hypertension, and venous varix proximal to the obstruction, especially in high-flow AVMs. The clinical manifestations of an insufficient or failing venous collateral circulation include:

i) Symptoms of mass effects or cranial nerve palsies caused by mechanical compression of the brain or cranial nerves by the venous varix.

ii) Seizures or progressive neurologic deficits caused by venous congestion of normal brain parenchyma.

iii) Haemorrhage because of AVM rupture, caused by venous hypertension.[17,20]

CLASSIFICATION OF CEREBRAL AVM

The most widely accepted classification scheme was the one proposed by Spetzler and Martin in 1986 and is primarily a directive for the surgical management of AVM. This classification compartmentalises cerebral AVM into six grades on the basis of the size, venous drainage and eloquence (Table 2) and has become entrenched as a common parlance among all stake holders in AVM management. It was established to grade AVMs according to degree of surgical difficulty and risk of surgical morbidity and mortality.

Table 2. Spetzler Martin (SM) grading:

Lesion characteristics	**Number of points**
A. Size	
Small (< 3 cm)	1
Medium (3 – 6 cm)	2
Large (> 6 cm)	3
B. Location	
Non-eloquent site	0
Eloquent site*	1
C. Pattern of venous drainage	
Superficial only	0
Any deep	1

[*eloquent brain: sensorimotor, language and visual cortex; hypothalamus and thalamus; internal capsule; brain stem; cerebellar peduncles; deep cerebellar nuclei]

CLINICAL PRESENTATION

The most common clinical presentation of BAVM is with haemorrhage. Other presentations include seizure, neurological deficit or headache. Incidental detection of AVMs on neuroimaging constitute is only 0.05%.

Haemorrhage

Haemorrhage is the initial manifestation of the disease in approximately 50% of patients with an AVM with reported annual risk of bleed amounting to 2-4% per year. Prior bleed significantly increases the propensity to subsequent haemorrhage with reported risk of re-bleed in the first year rising to between 6 -18%. In subsequent years the risk for bleed returns to the base line of 2-4% per year.[48] Patients who present with haemorrhage have significant 10% mortality and 20-30% morbidity, making intervention imperative.[49]

There is increasing evidence, that the incidence of haemorrhage is higher. It is not unusual to find old haemorrhagic areas on MR images or to observe small chronic haemorrhage during microsurgical removal of AVM in patients, in whom these events have not been detected clinically.[50] It has been postulated, that episodes of acute headaches, seizures or other neurological symptoms may represent haemorrhages. The prevalence of silent intralesional microhaemorrhage, that is asymptomatic bleeding in the nidal compartment, as determined by imaging evidence of bleeding before the outcome events is high in brain AVM and associated with increased risk of symptomatic intracranial haemorrhage.

Seizure

Seizures are the second most frequent presenting symptom of cerebral AVM, reported to occur in 30% of patients. In the prospective study of Ondra *et al.,* patients with AVM related haemorrhage and patients with epilepsy had similar long-term morbidity and mortality.[51] Seizures may also be a clinical manifestation of minor haemorrhage.

Headache

Headache not associated with an acute haemorrhage is a relatively frequent complaint of patients with AVM. AVM associated headache may or may not present with other symptoms. 'Intractable, unilateral headache should increase suspicion for brain AVM and prompt MRI evaluation' according to a review. According to the International Classification of Headache Disorders (ICHD-3) diagnostic criteria for AVM related headaches, they " have a clinical course that parallels that of a coexisting AVM in terms of temporality, severity, and location".

Neurological symptoms or deficits

Neurologic deficits not associated with present or previous haemorrhage occur less frequently than bleed or seizures. Focal neurologic deficits such as hemiparesis, aphasia without hemorrhage are seen as initial symptom of brain AVM in 1%–40% of patients.

NEUROANGIOGRAPHIC INVESTIGATIONS

Initial comprehensive neuroangiographic investigation of a brain AVM prior to suitable treatment decision including endovascular superselective catheterization and embolization of the AVM nidus, should provide following informations:

1) The arterial territory or territories involved into the supply of the AVM.

2) The individual feeding arteries.

3) The arterial supply of normal brain proximal, around and distal to the AVM.

4) Arterial high flow angiopathic changes: (a) arterial enlargement, dolicho-ectatic arteries, loops and kinking; extra-and/or intracranial; (b) isolated or multiple arterial stenosis, moya-moya-like changes; (c) proximal and/or distal flow-related aneurysms.

5) Gross assessement of the AVM nidus: (a) size and shape; (b) compact or diffuse; (c) plexiform and/or fistulous composition; (d) intranidal vascular cavities; (e) flow conditions.

6) Venous territory or territories involved in the drainage of the AVM.

7) Individual draining veins.

8) Venous high-flow angiopathic changes: (a) venous stenosis with or without venous collateral circulation; (b) venous varix; (c) venous occlusion; (d) dural sinus high-flow with secondary cortical arteriovenous shunt.

9) Venous anatomic variations; persisting embryonic veins.

10) Venous drainage of the normal brain.[52]

Digital Subtraction Angiography

DSA is the reference standard for the evaluation and characterization of brain AVMs. Its unsurpassed spatial and temporal resolution allow it to readily delineate the arterial supply, nidus, and venous drainage of an AVM and to depict hemodynamic factors, such as the degree of arteriovenous shunting, which are largely inapparent on noninvasive imaging.

DSA has been considered to be the criterion standard because of excellent depiction of cerebrovascular anatomic structures with high image contrast and spatial resolution. However, it is often difficult to determine the relationship between multiple overlapping vessels from 2D projectional images. Furthermore, small vessels may be obscured when they are adjacent to large areas of opacification. When complex vascular structures are being imaged, it may be necessary to make multiple acquisitions at various angles to provide adequate visualization. However, multiple acquisitions result in increased radiation exposure to the patient and repeated injections of contrast material.

3D Rotational Angiography (3D RA)

Rotational angiography is a medical imaging technique based on X-ray, that allows to acquire CT-like 3D volumes during hybrid surgery or during a catheter intervention using a fixed C-Arm. The fixed C-Arm thereby rotates around the patient and acquires a series of X-ray images that are then reconstructed through software algorithms into a 3D image.

In order to acquire a 3D image with a fixed C-Arm, the C-Arm is positioned at the body part in question so that this body part is in the

isocenter between the X-ray tube and the detector. The C-Arm then rotates around that isocenter, the rotation being between 180° and 360° (depending on the equipment manufacturer). Such a rotation takes between 5 and 20 seconds, during which a few hundred 2D images are acquired. A software then performs a cone beam reconstruction. The resulting voxel data can then be viewed as a multiplanar reconstruction, i.e. by scrolling through the slices from three projection angles, or as a 3D volume, which can be rotated and zoomed.

According to the literature, 3D RA is used mostly for the assessment of cerebral aneurysms. As 3D RA can provide substantial additional information on BAVM some centers perform 3D RA routinely for BAVM exploration prior to definitive management.[53] Such use of contrast is well tolerated even in the pediatric population.[54] A single 3D RA acquisition enables assessment of the entire AVM conformation and can eliminate multiple oblique angiography injections, thereby helping to decrease the overall contrast load used for angiographic explorations. Furthermore, the patient's radiation dose is reduced, as the 3D RA radiation dose is significantly lower than that of biplanar DSA, especially with the use of a flat-panel detector.[55,56]

COMPARISON OF 2D DSA AND 3D RA

2D DSA has been routinely performed as the initial comprehensive neuroangiographic evaluation of the brain AVM. Despite its usefulness in demonstrating the general vascular features of an AVM, selective 2D DSA of the internal carotid (ICA), external carotid (ECA) and vertebral arteries has significant limitations. Overprojection of early draining veins on arterial feeders may obscure visualization of small feeding arteries as well as small flow related aneurysms located in proximity to the nidus.

The nidus itself frequently obscures the intranidal aneurysms, pseudoaneurysms, venous aneurysms or varices and origin of the draining veins. Smaller direct arteriovenous fistulae may remain undetected on selective angiographic studies. In addition, because of different haemodynamic conditions in different parts (compartments) of an AVM, some small accessory draining veins may not be visualized at all.

Superselective catheterization and evaluation of the AVM is usually carried out during embolization. Selective angiographic studies are used for planning the superselective endovascular microcatheterization of the AVM nidus. Usually one or several feeding arteries are superselectively catheterized and embolized in one session. Appropriate selection of feeding artery for superselective microcathetrization and the microcathetrization sequence of several feeding arteries in a single session are important factors for successful embolization of a given AVM.

With the advent of 3D RA, the technique has been predominantly utilized for assessing the cerebral aneurysms.

Few comparative studies have been carried out in recent past between DSA and 3D RA in evaluation of intracranial aneurysms. Some researchers have shown that 3D RA is more sensitive for depiction of aneurysms than is DSA.[57]

Takeshi *et al.,* assessed 2D DSA and 3D RA for the overall image quality, presence of aneurysm, presence of aneurysmal lobulation, visualization of aneurysmal neck and relationship to adjacent vessels in a consecutive series of thirty six patients with forty aneurysms. 3D RA was found better to evaluate the morphologic characteristics of an aneurysm from multiple views with the use of variable reconstruction techniques,

such as multiplanar reconstruction, maximum intensity projection (MIP), shaded surface display (SSD), and volume rendering. Three-dimensional DSA was found to more clearly depict the subtle angiographic abnormalities.[58]

In the study titled 'Three-dimensional digital subtraction angiography *vs* two-dimensional digital subtraction angiography for detection of ruptured intracranial aneurysms: A study of 86 aneurysms' Masatoue *et al,* have shown that 3D-DSA was more sensitive for detection of smaller aneurysms. Also the 3D enabled a good analysis of the relationships among vascular structures. 3D-DSA had greater advantage in detecting cerebral aneurysms that were <5 mm in size.[57]

Integrating 3D RA into gamma knife radiosurgery treatment planning for brain AVM, Hirotaka *et al*, in their study of twenty five patients, showed better dose planning and treatment response owing to clearer visualization of the nidus as compared to 2D DSA.[59]

Precise mapping of the AVMs was achieved with identification of each feeding artery, as well as arteries at the border of the AVM, by combined analysis of the vessels of interest on anteroposterior and lateral views of the angiogram and the 3D RA in a pilot study by Raphael *et al*. The processed 3D RA images were static, ignoring critical information of the angiogram, especially superimposition of the veins obscuring nidus details. Dynamic datasets from 2D angiography was found helpful and complemented 3D RA images for guiding microcatheter navigation.[60]

X. Combaz *et al*, in a prospective study titled 'Three-dimensional rotational angiography in the assessment of the angioarchitecture of brain arteriovenous malformations' included 72 patients who had undergone conventional DSA and 3D RA for pretherapeutic assessment of BAVM

prior to radiosurgery.[53] Dimensional criteria, arterial-feed patterns, venous drainage, points of weakness and vascular densities of the nidus and shunt zone were studied with the aim to assess whether or not 3D RA might improve the assessment of BAVM. In this study, 3D RA detected all AV shunts by revealing abnormal venous enhancement. In addition, the technique provided significant help for volumetric estimations, extraction of arterial feeders and origins of draining veins, and analysis of the 3D conformation of the nidus. Furthermore, 3D RA detected significantly more points of weakness, such as intranidus aneurysms and venous anomalies. In the study, these points of weakness were not significantly linked to a bleeding history.

Another advantage of 3D RA was that it obviates the need for multiple superselective catheterization to characterize the nidus and feeding pattern, especially during the planning of endovascular procedures.[61] As a result, the duration and irradiation of pretherapeutic angiography are both likely to be reduced. However, superselective catheterization, the most accurate technique for evaluation of BAVM, is still needed for the most complex lesions.[62]

We intend to compare between 2D DSA and 3D RA in brain AVM to analyze the arterial feeders, nidal pattern, detection of flow related aneurysms, arterivenous fistulous components, and various high-flow angiopathies. Such a comparative study would be helpful to depict the strengths or limitations of 3D RA for evaluation of brain AVM.

ANGIOGRAPHIC MARKERS OF CLINICAL MANIFESTATIONS IN BAVM

Haemorrhage

Salient angiographic features with statistically significant increased incidence of haemorrhage in AVM as correlated from several studies over the years include:

1) Prior haemorrhage
2) Deep location
3) Exclusive deep drainage
4) Associated flow related aneurysm
5) Infratentorial location
6) Stenosis or occlusion of draining veins
7) Small size
8) MCA perforator feeders

Daniel H. Sahlein *et al*, in a retrospective study, from 1996 to 2006, with one hundred twenty two brain AVM patients reported single venous drainage anatomy, multiple draining veins and a venous stenosis and AVMs with associated aneurysms were more likely to present with hemorrhage. Whereas, those with multiple draining veins and without stenosis had diminished association with hemorrhage presentation. These findings were confirmed in both univariate and multivariate models.[3]

Michael J Ellis *et al*, studied a cohort of 135 children with AVMs from 2000 to 2011. 86/135 (63.7%) children presented with hemorrhage.

AVM location, morphology and the presence of associated aneurysm, venous varix, draining vein stenosis and single draining vein were not significantly associated factors. After multivariate analysis, smaller AVM size, exclusive deep venous drainage and infratentorial location were the specific angioarchitectural factors independently associated with initial hemorrhagic presentation in children with AVMs.[63]

Seizure

Various factors associated with increased risk of seizures in unruptured brain AVM patients include:

1) Location in temporal > parietal > frontal lobes, involvement of motor-sensory strip
2) Rerouting of venous drainage from the AVM
3) Venous hypertension
4) Fistulous component in the nidus
5) Size larger than 3 cm
6) Long pial course of draining vein

The incidence of seizures is particularly high in AVM of temporal lobe, those involving the motor-sensory strip and in younger patients.[64] Berenstein and Lasjaunias in a retrospective analysis of angiographic data of patients with AVM presenting with epilepsy, suggested that rerouting of venous drainage from the AVM through a vein that previously drained normal brain and the associated venous hypertension as major cause of epilepsy.

J.J.S. Shankar *et al*, analyzed 33 patients with unruptured BAVMs with seizures and 45 patients with unruptured AVMs without seizures in a retrospective review of four BAVM database from 2000 to 2009. Nidus size larger than 3 cm presented significantly more often with seizures. The frontal, temporal, and parietal locations of the BAVMs were significantly associated with the occurrence of seizures. Three arterial features (fistulous component, arterial dilation, and perinidal angiogenesis) were evaluated. These 3 features indicate high flow throughput of the AVM with subsequent perinidal hypoxemia. Of these 3 features, the presence of a fistulous component had the strongest association with seizure occurrence. Of the 4 investigated venous features (long pial course of the draining vein, pseudophlebitic pattern, venous outflow stenosis, and venous ectasia), 2 (long pial course of the draining vein and venous outflow restriction) demonstrated high predictive value for presentation as seizures.[65]

Dale Ding *et al*, in their study titled 'Cerebral Arteriovenous Malformations and Epilepsy: Predictors of Seizure Presentation' noted that amongst 1007 patients with brain AVM, 229 patients (23%) presented with seizures. Larger nidus diameter and cortical locations were found to be the independent predictors of seizure presentations. Frontal, temporal and parietal lobar AVMs have similar incidences (approximately 35% cases) of seizure presentation; whereas occipital lobe has lesser incidence of 21%. Amongst the noncortical locations, insula has significantly higher incidence (32%) of seizures.[66]

A large AVM may be more likely to present with seizures because the overall "sump effect" of the AVM may be more prominent, compared with a small AVM.

Deeply located BAVMs may present with seizure due to the interference of the venous drainage of mesial temporal lobe structures.

Factors related to high flow such as dilation of the feeding artery and a fistulous component in the nidus can give rise to relative arterial functional steal in the region of the nidus. This arterial steal with subsequent local hypoxemia may lead to an increased perinidal angiogenesis with blood being rerouted from the normal brain tissue due to the sump effect of the BAVM. Hypoxemia leads to an increased activity of the vascular endothelial growth factor triggered by the hypoxemia inducible factor. The subsequent perinidal angiogenesis, in turn, extends the area of functional arterial steal to the adjacent cortex, resulting in a larger area of cortex being hypoxemic. Chronic hypoxemia can lead to gliosis, which, in turn, may trigger epileptic activity.

Venous congestion of normal brain tissue can be due to an increased inflow into the venous system (such as in fistulous lesions) or to a reduced outflow. Venous congestion may be accompanied by a cognitive decline or seizures. From an imaging point of view, the pseudophlebitic pattern (increased tortuosity of pial veins), delayed venous return of normal brain, venous rerouting, and secondary recruitment of pial superficial veins are the signs of venous congestion.

Mass effect is a rare pathomechanism that may result from large venous ectasia or the nidus proper compressing critical structures, and it may lead to seizures, neurologic deficits, and even hydrocephalus. The presence of venous ectasia was also found to be significantly associated with seizures.

Headache

Occipital AVM is most commonly associated with headache in 15% to 61% of cases and is often characterized by visual & migraine-like symptoms.

Several mechanisms involving trigeminovascular activation are often proposed in the literature as mechanisms underlying nonhaemorrhagic headache in patients with AVM:

- Increased intracranial pressure (ICP) is believed to possibly trigger headache by activating the trigeminal system at high pressures. Findings suggest that the buffering capacity against ICP may become overwhelmed due to the AVM, and patients with headache may be hypersensitive to small increases in ICP.

- Steal phenomena from the high-flow arteriovenous shunting in AVM may lead to headache; however this concept is controversial.

- Cortical spreading depression (CSD) may lead to headache via alterations within the meningeal vessels and resulting activation of the trigeminovascular system. Transient alterations in relative cerebral blood flow (rCBF) initiated by CSD within the occipital lobe secondary to AVM may cause headache and visual symptoms.[67]

Focal Neurological deficits or symptoms

Neurologic deficits not associated with previous haemorrhage occur less frequently than seizures or bleeding and may be caused by several mechanisms including steal effect of the AVM, decreased perfusion because of associated arterial stenosis, venous hypertension or

mass effect caused by compression of brain parenchyma by venous ectasia or varices.[20]

We intend to analyse and deduce the varied angiographic predictors for clinical presentations of haemorrhage, seizures, headache and neurologic deficits or symptoms in brain AVM.

MATERIALS AND METHODS

INTRODUCTION

This was a prospective study conducted from May 2017 to June 2019. Informed written consent was obtained from all the participants who were part of this study. Institutional ethics committee approval was obtained for the study.

Consecutive patients with brain arteriovenous malformations presenting to the SCTIMST neurosurgery, neurology and interventional radiology clinics by direct referrals and consultations from other departments were considered for inclusion. These patients underwent digital subtraction angiography as per standard guidelines followed in the institution as detailed below. 3D RA was obtained from the ICA or vertebral artery, from which the predominant arterial feeder or feeders to the AVM was seen to arise.

After data collection, statistical analysis was done to generate inferences.

INCLUSION CRITERIA

i) All consecutive patients with Brain arteriovenous malformations presenting to SCTIMST neurosurgery, neurology or radiology clinics.

ii) Minors and pregnant women were also planned for inclusion with strict compliance with the international protocol related to the radiation protection and DSA norms.

EXCLUSION CRITERIA

(i) Patients in whom appropriate data is not available on PACS

(ii) Clinical features like seizure, headache or neurodeficit attributed to other pathologies in unbled AVM

(iii) Patients with seizure related to clinically undetected chronic haemorrhage and related gliosis in AVM

(iv) Prior embolization, surgery, stereotactic radiosurgery or gamma knife radiosurgery of the brain AVM

FLOW CHART OF STUDY DESIGN

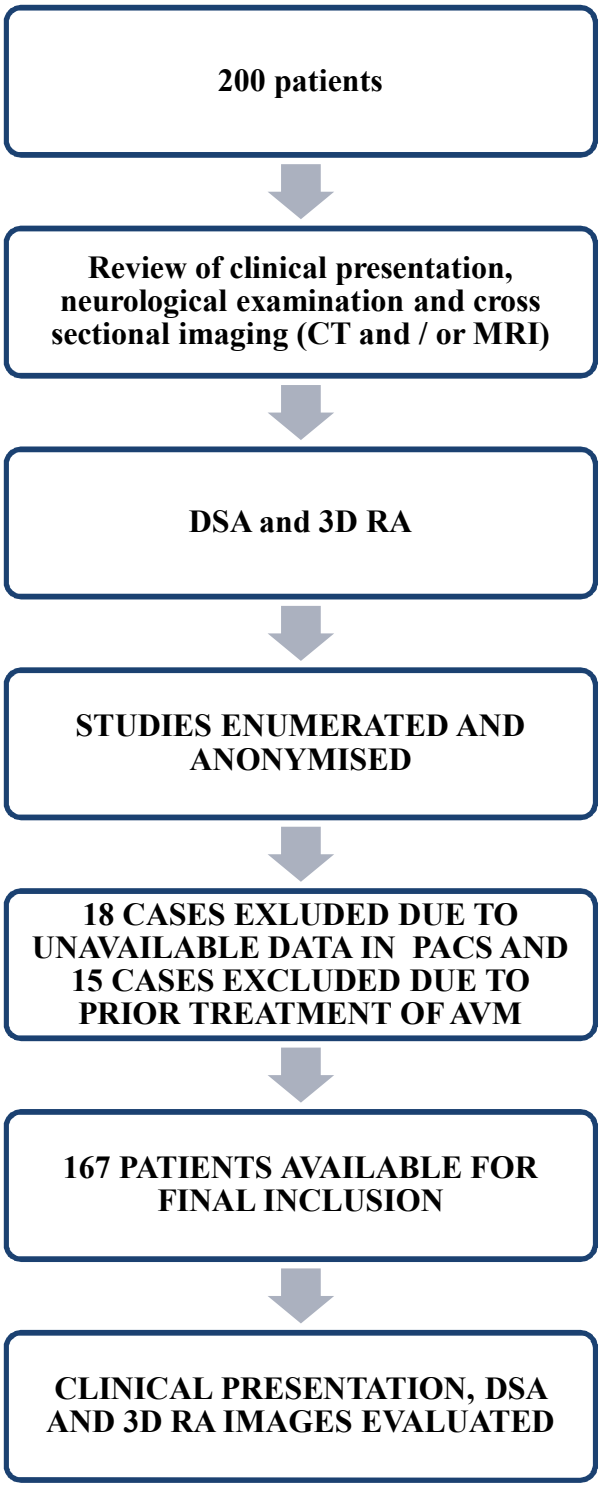

STUDY PROTOCOLS, TECHNIQUES AND PARAMETERS – DSA AND 3D RA

Consecutive patients with brain arteriovenous malformations considered for inclusion underwent detailed history taking, clinical – neurological examination, review of cross sectional images of CT scan and / or MRI of brain followed by Digital subtraction angiography including 3D RA as per the below stated protocol.

From clinical review and cross sectional imaging data; patients' presentation was considered as AVM with haemorrhage or unbled AVM with seizure / headache / neurological symptom or deficit.

After preliminary investigations of haemogram, serum electrolytes, renal function test, prothombin time, activated partial thromboplastin time and International Normalised Ratio (INR); patients underwent DSA including 3D RA in Interventional Radiology Suite at SCTIMST.

Bled AVM patients were undertaken for DSA & 3D RA following four to six weeks after the bleed or while clinically stable. Antiepileptic medication was used in patients who have had previous seizures and in those patients already on antiepileptic therapy or with a recent intracranial haemorrhage.

DSA including 3D RA was performed under local anaesthesia and continuous monitoring of ECG, blood pressure, pulse and oxygen saturation. General anaesthesia or sedation was reserved for children upto 12 years, uncooperative adult patients and in patients who were planned for embolization in the same sitting.

The neuroangiographic investigation of DSA and 3D RA was carried out on General Electric Innova biplane 1313 digital subtraction

equipment (generator of 1000 KW, RDL standard autoexposure). It has a detector size of 30 x 30 cm on both the planes. Angiography of the AVM was obtained with 4 frames per second (fps) rate in biplane and 7.5 fps in single plane. During 3D RA, the machine rotates by 192 degrees with a rotation time of five seconds. Single head pressure injector (MEDRAD PROVIS 5) was used to inject contrast in ICA or VA in all the cases. For ICA or VA injection, flow rate was kept at 3.5 ml/sec and pressure was kept at 300 PSI and 250 PSI respectively. In some of the cases with hypertrophic vertebral artery, pressure was kept at 300 PSI. Delay time for the pressure injection was set as per the visualization of the earliest arterial phase of the AVM in DSA; usually at 1.5 to 2 seconds in all cases.

Advantages of the biplane DSA system include improved contrast sensitivity, reduced volume of contrast agent used throughout the procedure, reduction of radiation exposure and reduced study time.

Non-ionic iodinated contrast agents (Iohexol or Iodixanol) were used exclusively for the endovascular investigation.

Angiograms were carried out using 6/7 F short sheaths via transfemoral route and 4 or 5 French diagnostic glide catheter (usually vertebral glide catheter). After securing the arterial sheath in common femoral artery, intra-arterial heparin was given at a dose of 60 to 80 IU per kg body weight. Selective angiograms were obtained from bilateral ICA, ECA and vertebral arteries (VA). Bilateral vertebral artery injections were obtained in cases of AVM with predominant posterior circulation arterial feeders. On average, a volume of 7 ml of contrast was injected for selective ICA, 5 ml for selective VA and 4 ml for selective ECA angiography. After assessing the DSA images, dominant arterial

feeders to the AVM were identified. AVM located fully in the territory of one anterior circulation territory was approached for 3D RA through the ipsilateral ICA. AVMs located in the posterior circulation territory (perforator, choroidal or pial posterior cerebral artery branches, anterior inferior cerebellar artery or superior cerebral artery) were approached through the dominant vertebral artery for 3D RA. 3D RA for AVM with dominant feeder as PICA was obtained from ipsilateral VA. AVM with dominant feeders from fetal PCA branches, was approached for 3D RA through ipsilateral ICA. 3D RA for multicompatmental AVMs with dominant feeders from both anterior & posterior circulation arteries or bilateral anterior circulation arteries were obtained from both ipsilateral ICA and dominant VA or bilateral ICA respectively.

The DSA and 3D RA images were then obtained from GE-PACS, anonymized and stored separately in numbered folders and analysed independently.

The images were assessed for following parameters:

1) The location of the AVM and whether located in eloquent area (determined from cross sectional images of CT or MRI, DSA and 3D RA)

2) Arterial feeders (determined from DSA and 3D RA): dominant feeder, supplementary feeder, any meningeal or dural feeder, any feeder from lenticulostriate or choroidal arteries or perforator arteries, direct or en-passage feeder types

3) Any hypertrophy of the arterial feeders (determined from DSA and 3D RA)

4) Size of the nidus including the maximum dimension (determined from DSA and 3D RA)

5) Nidus type: Diffuse / Compact / Sparse (analysed and tabulated separately from 2D DSA and 3D RA images)

6) Presence of fistulous component in the AVM (analysed and tabulated separately from 2D DSA and 3D RA images)

7) Presence and the number of intranidal aneurysm (analysed and tabulated separately from 2D DSA and 3D RA images)

8) Presence and the number of perinidal (distal extranidal) aneurysm (analysed and tabulated separately from 2D DSA and 3D RA images)

9) Presence and the number of flow related feeding artery aneurysm (analysed and tabulated separately from 2D DSA and 3D RA images)

10) Presence of perinidal angiopathy (determined from DSA and 3D RA)

11) Total number of draining veins (determined from DSA and 3D RA)

12) Total number of deep draining veins (determined from DSA and 3D RA)

13) Presence of any draining vein stenosis or occlusion (analysed and tabulated separately from 2D DSA and 3D RA images)

14) Presence of any venous rerouting or reflux (determined from DSA and 3D RA)

15) Presence of venous aneurysm or varix (determined from DSA and 3D RA)

16) Presence of ectasia of the draining veins (determined from DSA and 3D RA)

17) SM grade of AVM

STATISTICAL ANALYSIS

Data was entered in Microsoft excel for analysis. The analysis was carried out using SPSS version 21.0 and EpiInfo 7 software. For descriptive analysis, mean and SD was calculated for quantitative variables, and percentages or proportions were calculated for categorical data. Inferential statistics included application of Independent sample t test for difference between means, chi-square test for trend and Fisher's Exact test as applicable. A univariate model was constructed using all demographic and angioarchitectural characteristics. Categorical variables were assessed for dependence using 2×2 contingency tables. Multivariate logistic regression was carried out for variables, which showed significant association with outcome variables on univariate analyses. A *P* value of less than 0.05 was considered as statistically significant.

RESULTS

Demographics

This series consists of 167 patients with brain AVM. 107 patients (64.1%) were male and 60 patients (35.9%) were female. The age ranged between 2 and 63 years, with a mean age of 30 years and 17 patients being children below the age of 12 years.

Clinical Presentation

98 patients (58.7%) presented with intracranial haemorrhage or had a history of recent haemorrhage. Amongst unbled AVM patients, 42 patients (25.1%) presented with seizures, 14 patients (8.4%) with chronic headache and 9 patients (5.4%) with neurological symptoms or deficits. In 4 patients, (2.4%) the AVM was detected incidentally by CT or MR performed for non-specific or vague complaints.

Location

Summarised in Table 3. Frontal (19.2%) and parietal (18.6%) lobar AVM cases made up the commonest location of AVM in the present series. Multilobar involvement was seen in 17 patients (10%). Infratentorial location was seen in 12 patients (7.2%). Brainstem involvement was least common.

Table 3. BAVM locations.

AVM LOCATION	FREQUENCY	PERCENTAGE
FRONTAL	32	19.2%
PARIETAL	31	18.6%
TEMPORAL	27	16.2%
CEREBELLAR	11	6.6%
OCCIPITAL	9	5.4%
CHOROIDAL	9	5.4%
TEMPOROOCCIPITAL	9	5.4%
PARIETOOCCIPITAL	8	4.8%
CORPUS CALLOSAL/ PERICALLOSAL	8	4.8%
FRONTOPARIETAL	6	3.6%
BASAL GANGLIA	6	3.6%
INSULA	4	2.4%
THALAMIC	4	2.4%
PARIETOTEMPORAL	1	0.6%
PARIETO-TEMPORO--OCCIPITAL	1	0.6%
PONTINE	1	0.6%
TOTAL	167	

Feeding arteries

Pial feeding arteries were seen in all the AVMs with participation of the dural arterial system in 17 cases (10.2%). 25 AVMs (15%) were supplied by choroidal or perforating arteries including the lenticulostriate arteries. Hypertrophy of the feeding arteries was seen in 146 cases (87.4%).

Angiographic appearance of nidus

In the majority (42%) of cases, the nidus of the AVMs appeared angiographically as a compact vascular structure. Diffuse type AVM without clearly defined borders was seen in 29% of cases and in approximately 28% of cases, the nidus was sparse. No significant difference was seen between DSA and 3D RA in detecting the type of angiographic appearance of the AVMs as per the defined criteria (mentioned in discussion section).

Perinidal angiopathy

Perinidal angiopathy was found in 47 patients (28.1% cases).

Size

Maximum dimension of the nidus in the series ranged from 5 mm to 87 mm with mean of 30.8 mm.

Fistulous component in nidus

Direct arteriovenous communications (fistulae) were evident in 77 cases (46.1%) with DSA, significantly higher detection rate as compared to 3D RA (detection of 52 cases, 31.1%).

Flow related aneurysms

The number of aneurysms detected by 3D RA was significantly higher as compared to 2D DSA.

A total of 45 intranidal aneurysms in 32 brain AVMs was evident on DSA with significant false positive (six out of 32 cases, 18.7%) and false negative rates (36 of 135 cases, 26.7%). In 43 cases (25.7%), the presence or absence of intranidal aneurysm was indeterminate on DSA. 3D RA confirmed the presence of 94 intranidal aneurysms in 58 patients. Sensitivity of 2D DSA for detecting intranidal aneurysms is 43.1%, in other words, ability of 2D DSA to correctly diagnose those with intranidal aneurysms as established by 3D RA is 43.1%. Specificity of 2D DSA (ability of 2D DSA to correctly diagnose those without intranidal aneurysm as established by 3D RA) is 73.4%. (Table 4)

Table 4. Analyses of sensitivity and specificity of DSA for detecting intranidal aneurysms.

INTRANIDAL ANEURYSM : 2D DSA and 3D RA Crosstabulation

			3D RA - ANEURYSM		Total
			N	**Y**	
2D DSA ANEURYSM	N	Count	80	12	92
		% within 3D ANEURYSM	73.4%	20.7%	55.1%
	POSSIBLE	Count	22	21	43
		% within 3D ANEURYSM	20.2%	36.2%	25.7%
	Y	Count	7	25	32
		% within 3D ANEURYSM	6.4%	43.1%	19.2%
Total		Count	109	58	167
		% within 3D ANEURYSM	100.0%	100.0%	100.0%

The number of true intranidal aneurysms detected during interpretation was significantly higher with 3D RA (*n*=94) *vs* DSA (*n*=34) (*P*<0.001).

Both false positive and false negative rate of DSA for detecting the perinidal aneurysm was 20% (one out of five cases).

3D RA detected significantly higher number (21 cases, 12.6%) of AVM patients with feeding artery aneurysm as compared to DSA (14 cases, 8.4%) with *P* value < 0.05.

Venous findings and venous high-flow angiopathy

Significantly higher number of cases with draining vein stenosis was detected with 3D RA (36 patients, 21.6%) *vs* DSA (22 patients, 13.2%), *P* value < 0.001.

Venous varix or aneurysm was seen in 32 patients (19.2% cases). Presence of venous varix was observed in 19 bled and 13 unbled AVM patients respectively with no significant differences.

Venous reflux or rerouting was seen in 60 patients (35.9% cases).

SM grade

Of the 167 patients, 112 cases had SM grade of 2 and 3.

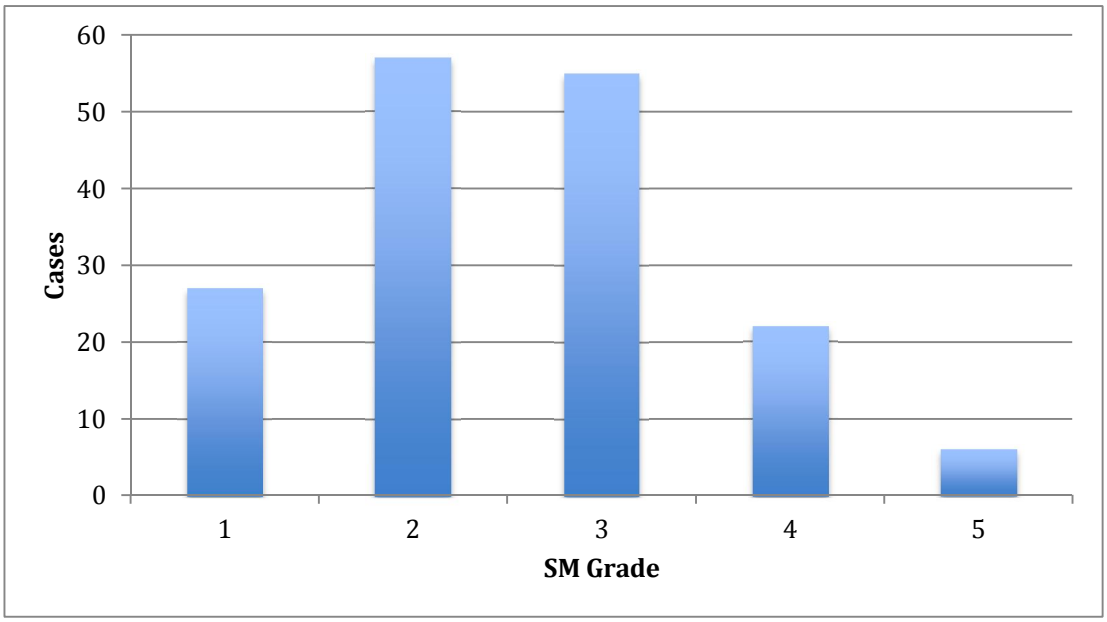

Angioarchitectural predictors for clinical presentations

Haemorrhage

Based on the results of the present study, the angioarchitectural characteristics those were significantly associated with haemorrhage includes:

i) AVM nidus size < 3 cm

ii) Location involving deep supratentorial region (basal ganglion, thalamus, callosal – pericallosal, intraventricular or choroidal), insula, operculum and infratentorial location of cerebellum or brainstem

iii) Sparse & compact nidus

iv) Predominant arterial feeders as small perforators, lenticulostriate or

choroidal arteries

v) Single superficial or deep draining vein

Statistically significant difference was noted between mean maximum diameter of the bled AVM (27.1 mm) and unbled AVM (36 mm) with $P < 0.001$. In multivariate analyses size < 3 cm was found as a significant independent predictor for haemorrhage ($P = 0.02$) (Table 6).

In the present study incidence of haemorrhage was significantly higher in deep or central brain AVM (85.7%), insula-opercular region (70%) and infratentorial location (66.7%) (Table 5). Superficial or cortical and subcortical AVMs had haemorrhagic presentations in 50% of the cases.

Table 5. Cross-tabulated data and Pearson Chi square test for significance of location as haemorrhagic risk factor in BAVM.

		BLED		Total
		N	Y	
LOCATION	BASAL GANGLIA /THALAMIC/CHOROIDAL	3	17	20
	CALLOSAL/PERICALLOSAL	1	7	8
	CEREBELLAR	4	7	11
	INSULA/OPERCULUM	3	7	10
	LOBAR	58	59	117
	PONS	0	1	1
	Total	69	98	167

Chi-Square Tests

	Value	df	Asymp. Sig. (2-sided)
Pearson Chi-Square	13.085[a]	5	.023

Brain AVMs with predominantly lenticulostriate or small perforator and choroidal arterial feeders (25 cases) were more likely to present with haemorrhage (23 cases, 92%) (P < 0.001). (Table 6)

Table 6. Pearson Chi square test for significance of choroidal or perforator arterial feeders as haemorrhagic risk factor in BAVM.

		BLED		**Total**
		N	**Y**	
Choroidal/ perforator feeder	N	67	75	142
	Y	2	23	25
Total		69	98	167

Chi-Square Tests

	Value	df	Asymp. Sig. (2-sided)	Exact Sig. (2-sided)	Exact Sig. (1-sided)
Pearson Chi-Square	13.461	1	.000		
Continuity Correction	11.893	1	.001		
Likelihood Ratio	16.108	1	.000		
Fisher's Exact Test				.000	.000
N of Valid Cases	167				

Deep brain and plexal location and perforator or choroidal arterial main feeders were found as independent predictors of haemorrhage in multivariate analyses ($P = 0.003$). (Table 7)

Haemorrhagic presentation was seen in 85% cases with sparse nidus pattern, 60% cases with compact nidus and in 32% cases with diffuse nidus and the difference in the nidus pattern between bled and unbled AVM subgroups was significant ($P < 0.001$).

Mean of total number of draining veins in bled and unbled AVM was 2.1 and 2.7 respectively with statistically significant difference ($P = 0.007$) between these two subgroups. Single draining vein was found as a risk factor for haemorrhage in the univariate analyses ($P <0.05$).

Significant negative correlation was seen between haemorrhage and presence of venous collateral rerouting in brain AVM ($P < 0.001$).

In this study, there was no statistically significant association of bled AVM with the presence of intranidal or perinidal aneurysms noted ($P = 0.3$) (Table 8). Venous stenosis, venous varix and SM grade were not independent predictors of haemorrhage.

Table 7. Results of the multivariate logistic regression analyses for predictors of haemorrhage.

Included Variables	**Significance (*P* value)**
Choroidal or Perforator arteries as main feeder	**0.003**
Size < 3 cm	**0.02**
Single draining vein	0.17

Table 8. Pearson Chi square test for significance of intranidal aneurysms as haemorrhagic risk factor in BAVM.

		BLED		Total
		N	Y	
3D RA detected intranidal aneurysm	N	48	61	109
	Y	21	37	58
Total		69	98	167

Chi-Square Tests

	Value	df	Asymp. Sig. (2-sided) (p value)	Exact Sig. (2-sided)	Exact Sig. (1-sided)
Pearson Chi-Square	.957	1	.328		
Continuity Correction	.661	1	.416		
Likelihood Ratio	.964	1	.326		
Fisher's Exact Test				.409	.208
N of Valid Cases	167				

Seizure

Angioarchitectural features found to be associated with clinical presentations as seizure in BAVM, in this study includes:

i) Size > 3 cm

ii) Diffuse nidus

iii) Presence of arteriovenous fistulous component

iv) Perinidal angiogenesis

v) Venous collaterals and rerouting

Cerebral AVMs presenting as seizures were significantly larger in size (mean maximum diameter of 36.1 mm).

Seizure in unbled AVM was seen in 42% cases with diffuse nidus, 27% cases with compact nidus and in only 2% cases with sparse nidus pattern and this distribution was statistically significant (Table 9).

Table 9. Pearson Chi square test for significance of pattern of nidus as risk factor for seizures in BAVM.

Crosstabulated data:

		SEIZURE		Total
		N	Y	
NIDUS	Compact	52	20	72
	Diffuse	28	21	49
	Sparse	45	1	46
Total		125	42	167

Chi-Square Tests

	Value	df	Asymp. Sig. (2-sided)
Pearson Chi-Square	21.325[a]	2	.000

Patients with fistulous nidus component were more likely to present with seizures (P = 0.003) (Table 10).

Table 10. Pearson Chi square test for significance of fistula as risk factor for seizures in BAVM.

Crosstabulated data:

		SEIZURE		Total
		N	Y	
FISTULA	N	75	14	89
	Y	50	28	78
Total		125	42	167

Chi-Square Tests

	Value	df	Asymp. Sig. (2-sided)	Exact Sig. (2-sided)	Exact Sig. (1-sided)
Pearson Chi-Square	8.981	1	.003		
Continuity Correction	7.942	1	.005		
Likelihood Ratio	9.066	1	.003		
Fisher's Exact Test				.004	.002
N of Valid Cases	167				

Brain AVMs with perinidal angiogenesis were more likely to present with seizures (P < 0.001) (Table 11).

Table 11. Pearson Chi square test for significance of perinidal angiogenesis as risk factor for seizures in BAVM.

		SEIZURE		Total
		N	Y	
Perinidal angiopathy	N	100	20	120
	Y	25	22	47
Total		125	42	167

Chi-Square Tests

	Value	df	Asymp. Sig. (2-sided)	Exact Sig. (2-sided)	Exact Sig. (1-sided)
Pearson Chi-Square	16.300	1	.000		
Continuity Correction	14.738	1	.000		
Likelihood Ratio	15.268	1	.000		
Fisher's Exact Test				.000	.000
N of Valid Cases	167				

Collateral rerouting of AVM venous drainage had significant association with seizure presentations ($P = 0.001$) (Table 12).

Table 12. Pearson Chi square test for significance of collateral venous rerouting as risk factor for seizures in BAVM.

		SEIZURE		Total
		N	Y	
VENOUS REROUTING	N	89	18	107
	Y	36	24	60
Total		125	42	167

Chi-Square Tests

	Value	df	Asymp. Sig. (2-sided)	Exact Sig. (2-sided)	Exact Sig. (1-sided)
Pearson Chi-Square	10.971	1	.001		
Continuity Correction[b]	9.774	1	.002		
Likelihood Ratio	10.651	1	.001		
Fisher's Exact Test				.001	.001
N of Valid Cases	167				

Deep supratentorial and infratentorial location, sparse nidus and predominant small perforator, lenticulostriate or choroidal arterial feeders had significant negative correlation with seizure presentations.

Flow related aneurysms, venous stenosis, venous varix and SM grade of AVM didn't have any significant association with seizure manifesations.

Among all the predictive factors for seizure, presence of fistula and perinidal angiogenesis were found to be significant independent predictors for seizure in multivariate logistic regression analysis (Table 13).

Table 13. Results of the multivariate logistic regression analyses for predictors of seizure.

Included Variables	Significance (*P* value)
Presence of fistula	**0.03**
Perinidal angiopathy	**0.01**
Diffuse nidus	0.12
Size > 3 cm	0.19
Venous rerouting	0.14

Headache

Presence of dural arterial feeders to the AVM, perinidal angiogenesis and higher SM grade (grade 3 to 5) were significantly associated with AVM related headache compared to those without headache (*P* value of 0.017, < 0.001 and 0.008 respectively) (Table 14-16).

Table 14. Pearson Chi square test for significance of dural arterial feeders as risk factor for headache in BAVM.

		HEADACHE		Total
		N	Y	
DURAL ARTERIAL FEEDER	N	140	10	150
	Y	13	4	17
Total		153	14	167

Chi-Square Tests

	Value	df	Asymp. Sig. (2-sided)	Exact Sig. (2-sided)	Exact Sig. (1-sided)
Pearson Chi-Square	5.653	1	.017		

Table 15. Pearson Chi square test for significance of perinidal angiogenesis as risk factor for headache in BAVM.

		HEADACHE		Total
		N	Y	
Perinidal angiopathy	N	116	4	120
	Y	37	10	47
Total		153	14	167

Chi-Square Tests

	Value	df	Asymp. Sig. (2-sided)	Exact Sig. (2-sided)	Exact Sig. (1-sided)
Pearson Chi-Square	14.157[a]	1	.000		
Continuity Correction[b]	11.917	1	.001		
Likelihood Ratio	12.473	1	.000		
Fisher's Exact Test				.001	.001
N of Valid Cases	167				

Table 16. Pearson Chi square test for significance of SM grade as risk factor for headache in BAVM.

		HEADACHE		Total
		N	Y	
SM GRADE	1	26	1	27
	2	57	0	57
	3	48	7	55
	4	17	5	22
	5	5	1	6
Total		153	14	167

Chi-Square Tests

	Value	df	Asymp. Sig. (2-sided)
Pearson Chi-Square	13.766	4	.008
Likelihood Ratio	16.731	4	.002
N of Valid Cases	167		

Neurological symptoms or deficits

Location of the AVM in brain parenchyma was determinant of the possible focal neurological symptoms or deficits. Unbled AVM with clinical manifestations as focal neurological deficits or neurological symptoms other than headache and seizure were more likely to involve the 'eloquent' brain area ($P = 0.013$) (Table 17).

Table 17. Chi square test for significance of eloquent brain location as risk factor for focal neurological symptoms or deficits (FND) in BAVM.

		FND		Total
		N	Y	
ELOQUENCE	N	85	1	86
	Y	73	8	81
Total		158	9	167

Chi-Square Tests

	Value	df	Asymp. Sig. (2-sided)	Exact Sig. (2-sided)	Exact Sig. (1-sided)
Pearson Chi-Square	6.212	1	.013		
Continuity Correction	4.620	1	.032		
Likelihood Ratio	6.960	1	.008		
Fisher's Exact Test				.016	.014
N of Valid Cases	167				

Two patients of cerebellar AVM had presented with speech disorder and cerebellar signs of ataxia and incoordination. A patient with right cerebellar AVM was symptomatic with right-sided tinnitus. Two patients with unbled thalamic AVM had contralateral mild hemiparesis and paraesthesia. Proptosis of left eye was seen in one patient with parietal AVM with venous rerouting into the left cavernous sinus and retrograde flow into left superior orbital vein.

REPRESENTATIVE CASES

Section I. Comparison of 3D RA and 2D DSA

Case 1.

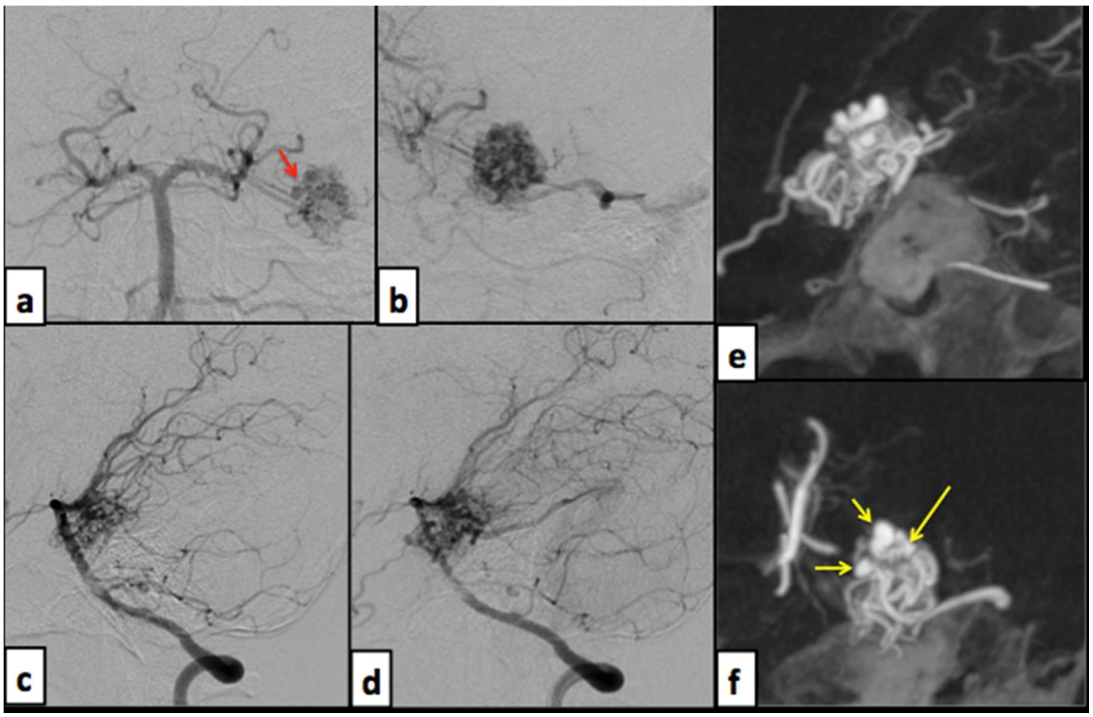

Sagittal and coronal reconstructed images of 3D RA (e and f) from left vertebral artery demonstrating three intranidal aneurysms (yellow arrows) with clarity, whereas analyses of left vertebral artery DSA arterial phase sequential images (a and b, anteroposterior projection; c and d, lateral projection) could conclusively identify only one aneurysm (red arrow) in this 13 years old boy with bled compact nidus AVM involving left posterior temporal lobe.

Case 2.

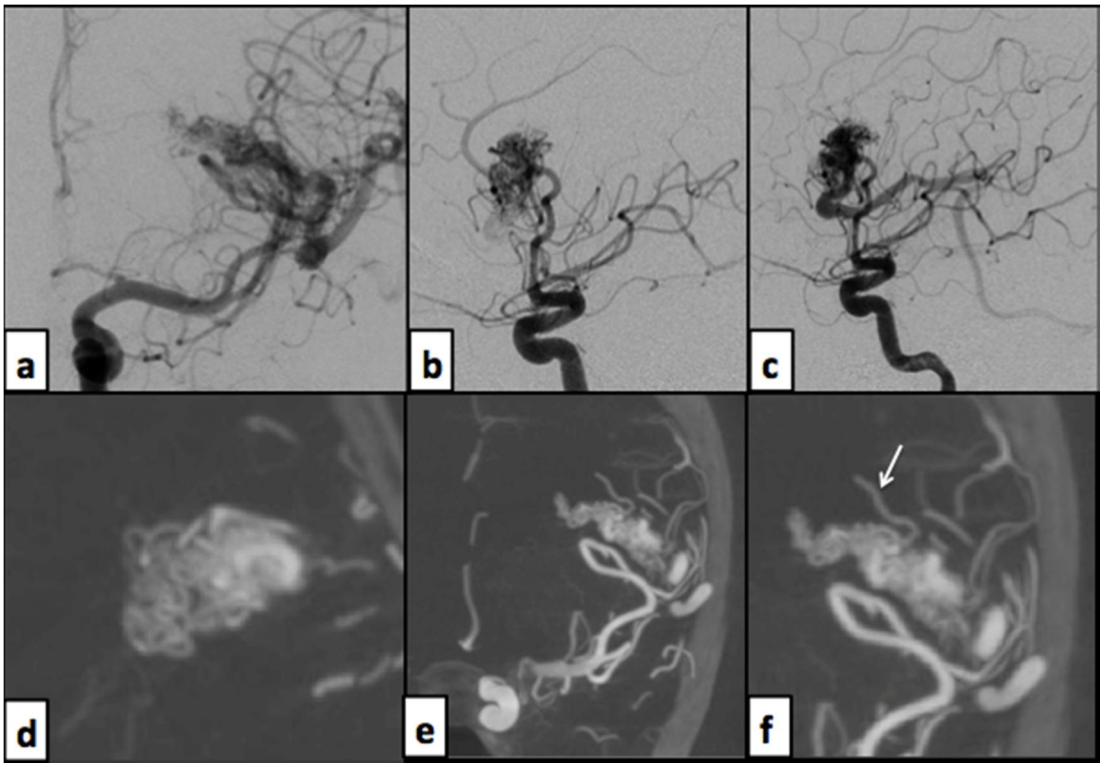

Left insular bled AVM in a 19 years old male patient. a, Anteroposterior; b and c, lateral images of left ICA DSA in arterial phase and 3D RA axial (d) and coronal (e, f) images demonstrating compact appearance of the nidus with plexiform shunting in the nidus. Left MCA insular branch appears as a direct feeder in DSA, but 3D RA indubitably showed the en-passage type (white arrow) of the feeder.

Case 3.

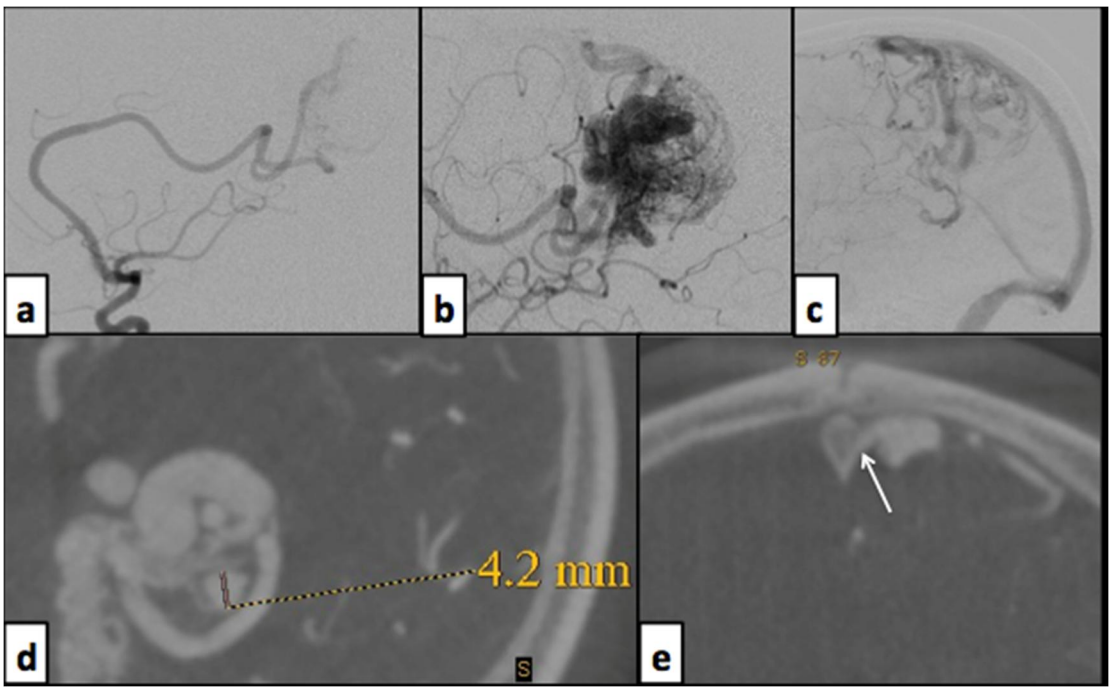

3D RA images (d, axial and e, coronal) demonstrating a 4 mm intranidal aneurysm and venous outflow stenosis (white arrow). Analyses of 2D DSA (a, b, and c, lateral projection of serial sequential left ICA angiography) didn't reveal any aneurysm or draining vein stenosis of the left parietal bled AVM in a 31year old man.

Case 4.

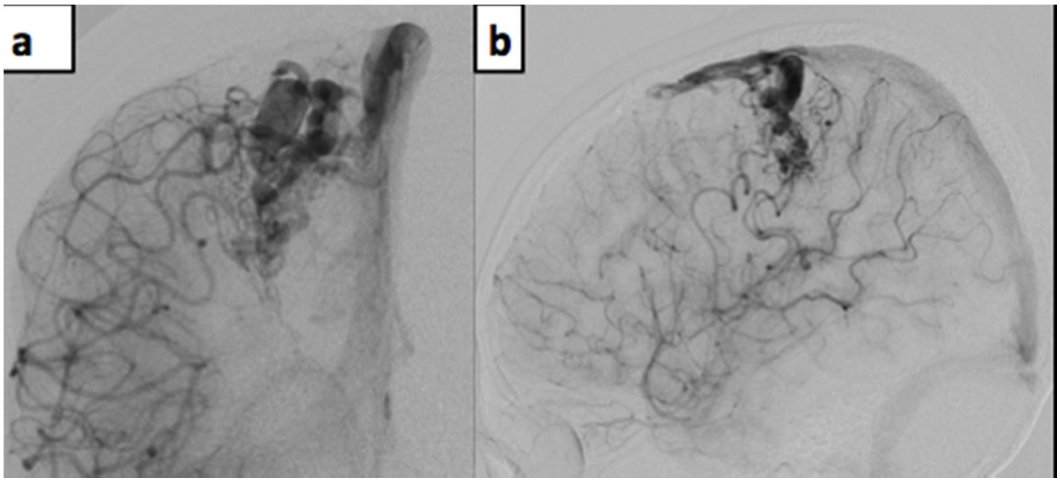

A case of perirolandic bled AVM (sparse nidus AVM with an intranidal aneurysm and single draining vein) in a 16 years old girl. 3D RA coronal image (c) demonstrating the venous stenosis (red arrow) with a proximal venous varix. The stenosis was not depicted in the 2D DSA (a, frontal and b, lateral projection of right ICA angiogram.

Case 5.

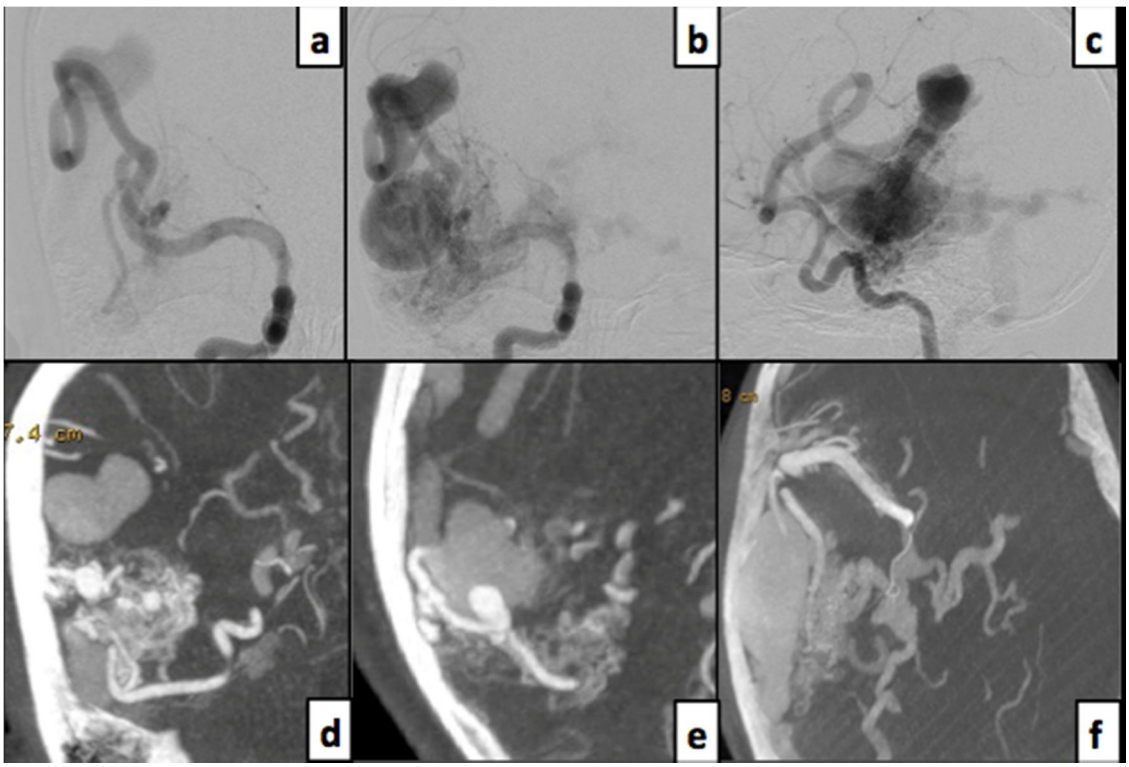

Right posterior temporal bled AVM in a 19 years old female patient. Anteroposterior (a, b) and lateral projections (c) of right ICA DSA revealed the fistulous AVM with a venous varix. 3D RA images (d, e and f) demonstrating multiple intranidal aneurysms (not visualized on 2D DSA) and venous collateral rerouting and deep venous drainage (not depicted clearly in 2D DSA of this case).

Case 6.

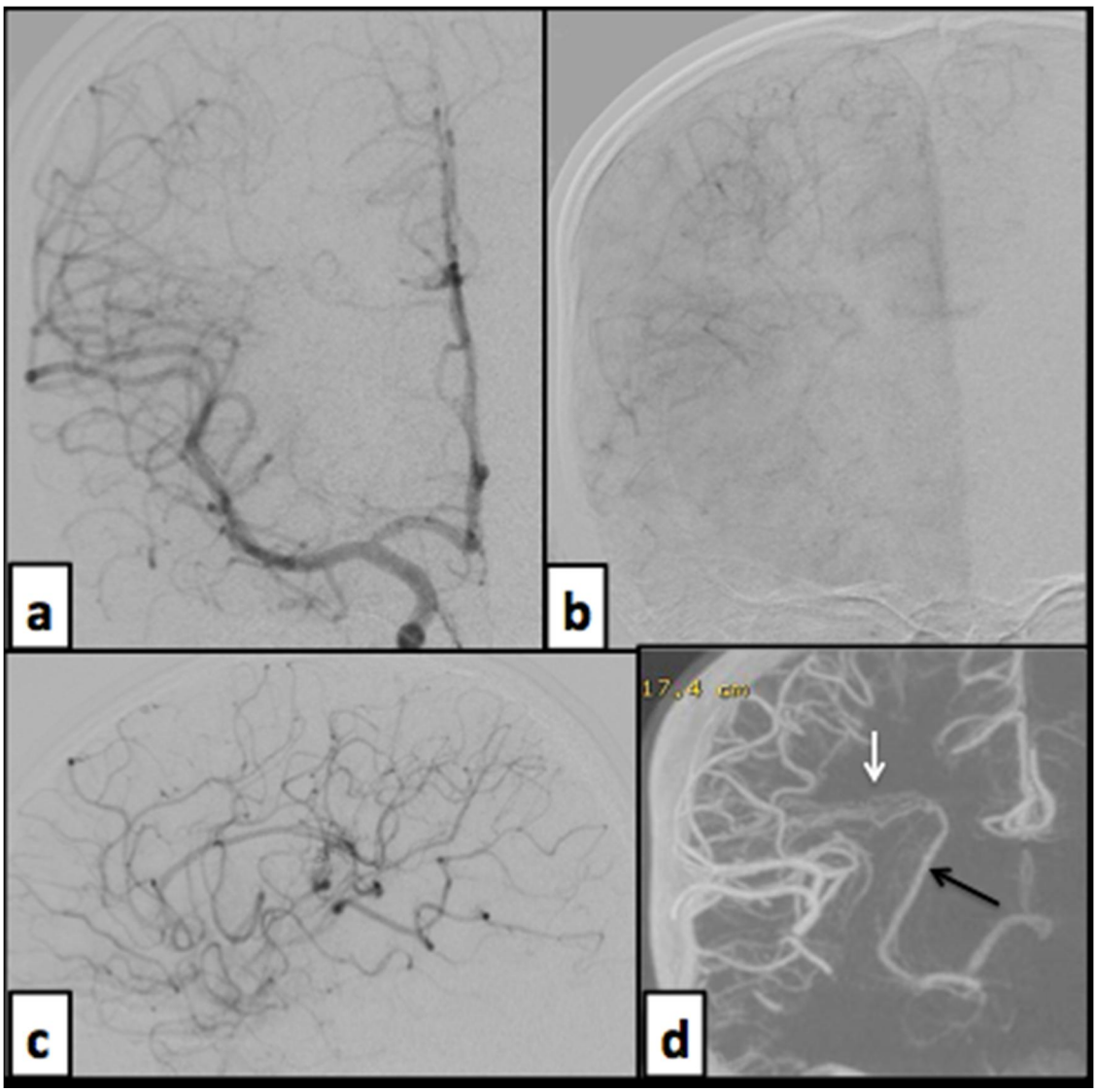

Importance of 3D RA in detecting small or subtle slow flow AVMs.

6 years old boy underwent DSA to investigate the cause for focal intracranial haemorrhage in right corona radiate. a,arterial phase; b,capillary phase (anteroposterior projection) DSA images of right ICA angiography revealed no obvious abnormalities. c, Lateral image of ICA angiogram demonstrating a tiny central area of suspicious vascular abnormality. d,3D RA coronal MIP reconstructed image clearly depicting a sparse nidus right subcortical small AVM with medullary arterial feeders and a single deep draining vein.

Case 7.

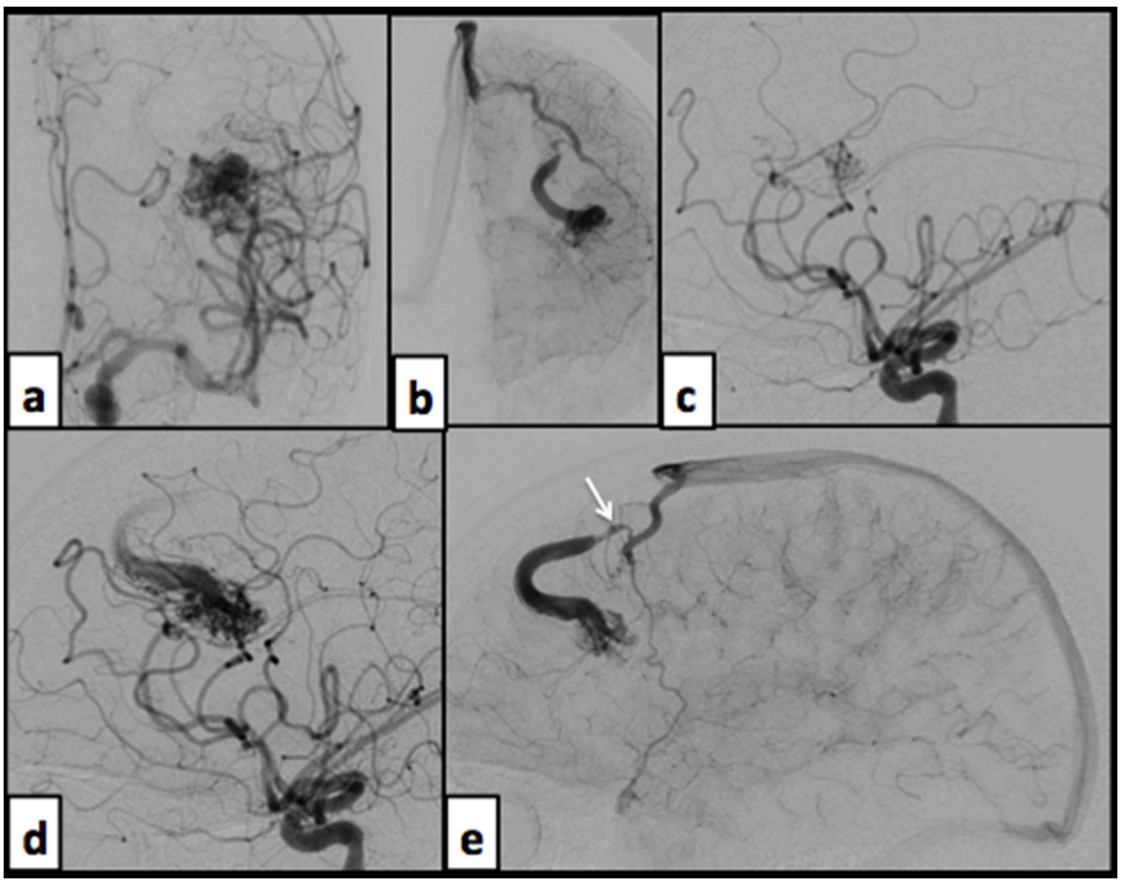

57 years old male patient was detected with an unbled left frontal AVM while investigated for an episode of syncope. Serial DSA images (a to e) of left ICA angiogram revealed indirect evidence (prompt appearance of the single superficial frontal cortical draining vein within 0.5 second of early arterial phase) for presence of fistulous component. White arrow - Venous outflow stenosis.

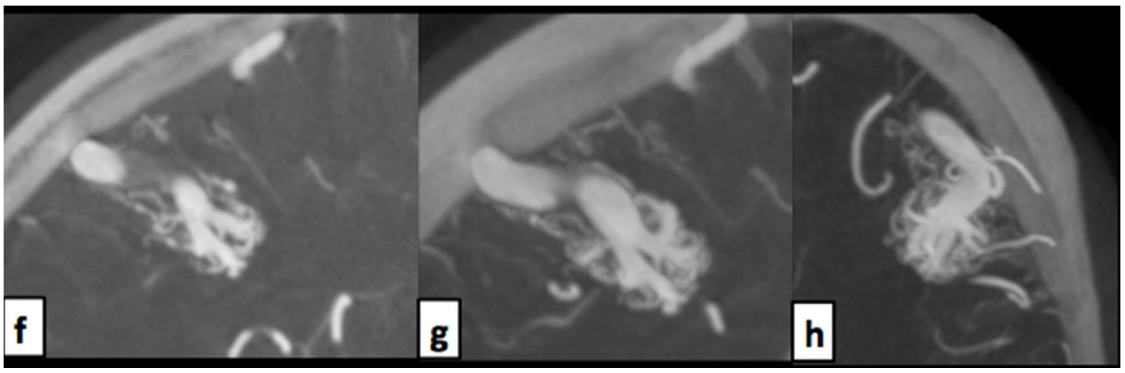

3D RA images (f and g, sagittal; h, axial) demonstrating the compact plexiform nidus and emergence of the ectatic draining vein from the vascular conglomerate. Evidence of fistula (feeding arteries ending directly into a vein or veins) was not seen.

Presence of fistulous components in such cases can only be confirmed by superselective angiography.

Section II. Angioarchitectural predictors for clinical presentations in BAVM

A. Haemorrhage

Case 8.

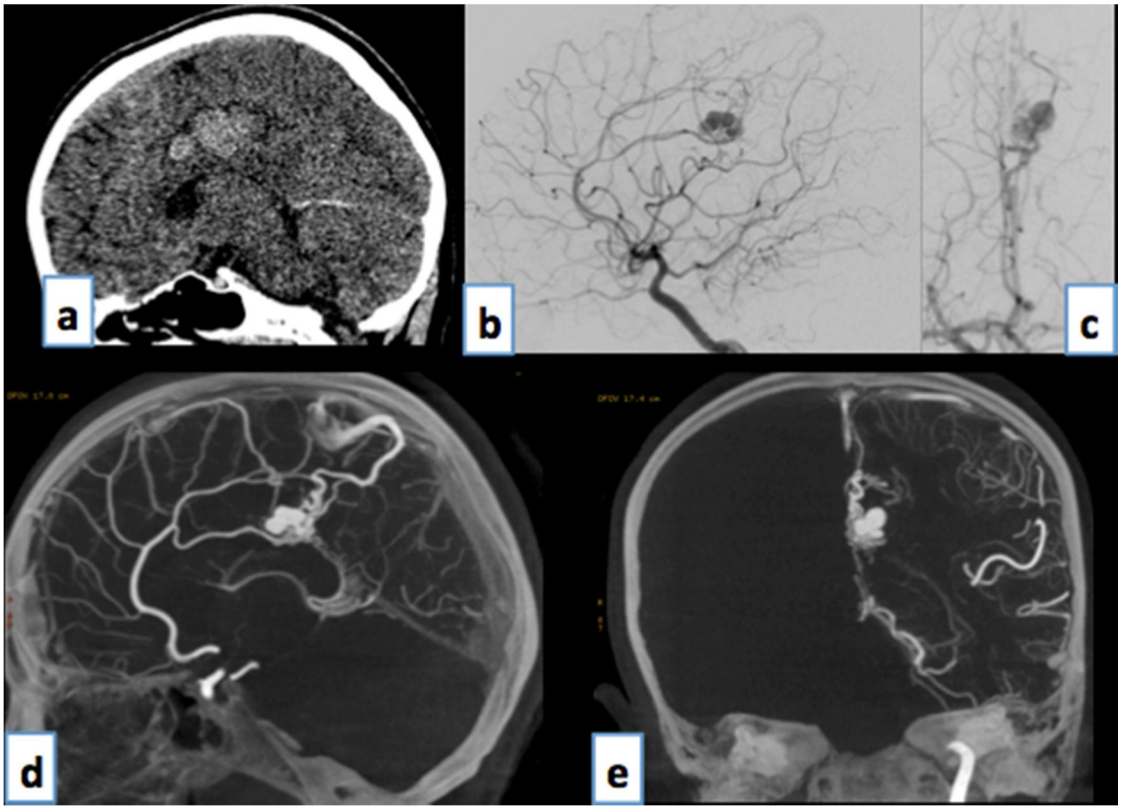

Increased incidence of distal flow-related aneurysms in bled AVM. 12 years old girl with left pericallosal haemorrhage (a, CT image). b and c, Lateral and anteroposterior (AP) mid arterial phase images of left ICA angiogram demonstrating sparse nidus pattern of AVM and nidal arterial aneurysm. d and e, Sagittal and coronal reconstructed images of 3D RA more precisely depict the lobulated nidal aneurysm. The irregular lobulated 8 x 6 mm sized aneurysm was the likely source of haemorrhage and a potential risk factor for rebleed in future.

Case 9.

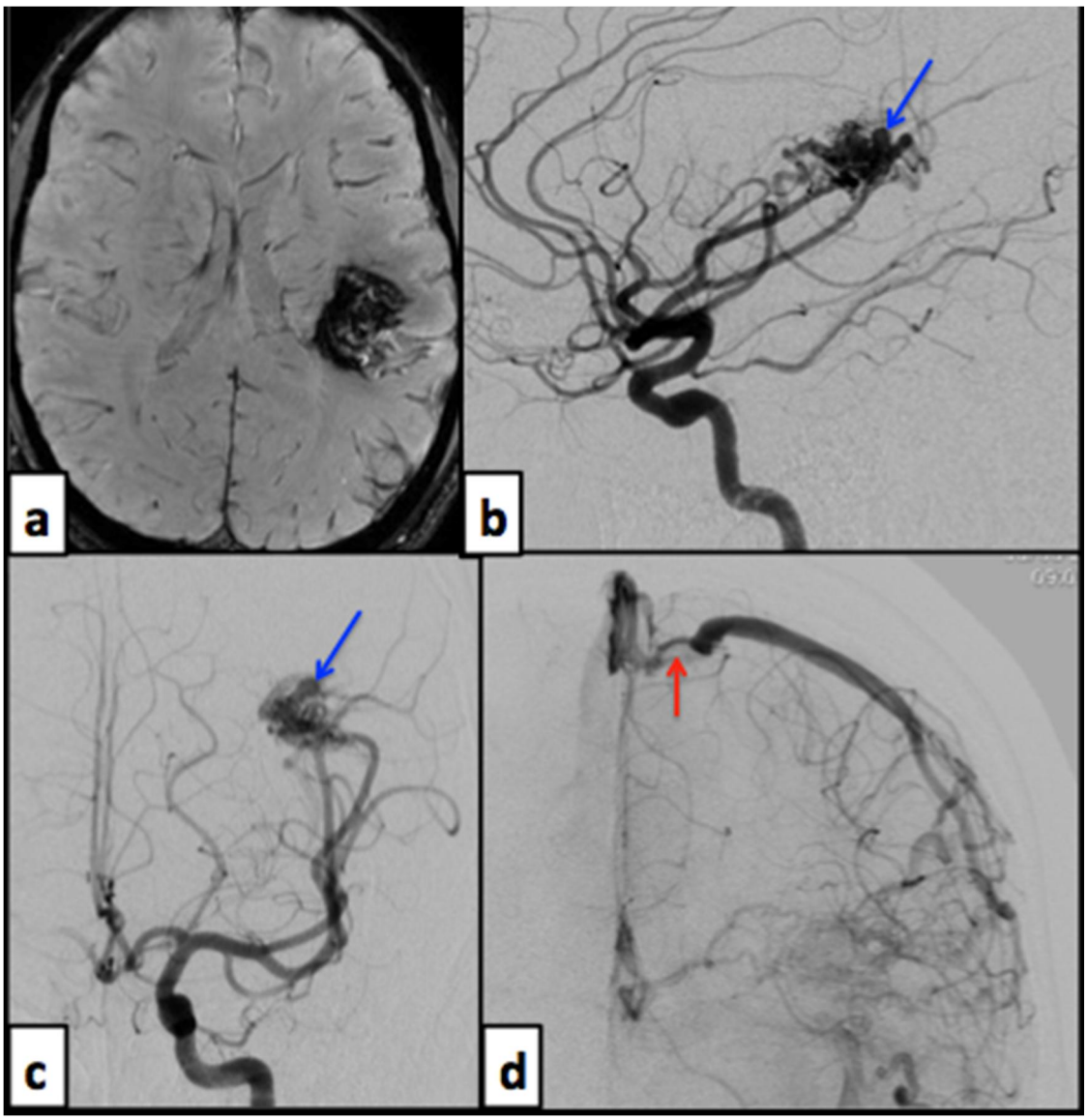

a, Susceptibility weighted MRI demonstrating left parietal opercular haemorrhage in a 22 years old man. b and c, Lateral and frontal projections of left ICA DSA in arterial phase depicting the compact nidus AVM with an intranidal aneurysm (blue arrow). d, DSA image of venous stenosis (red arrow) of the parietal cortical draining vein.

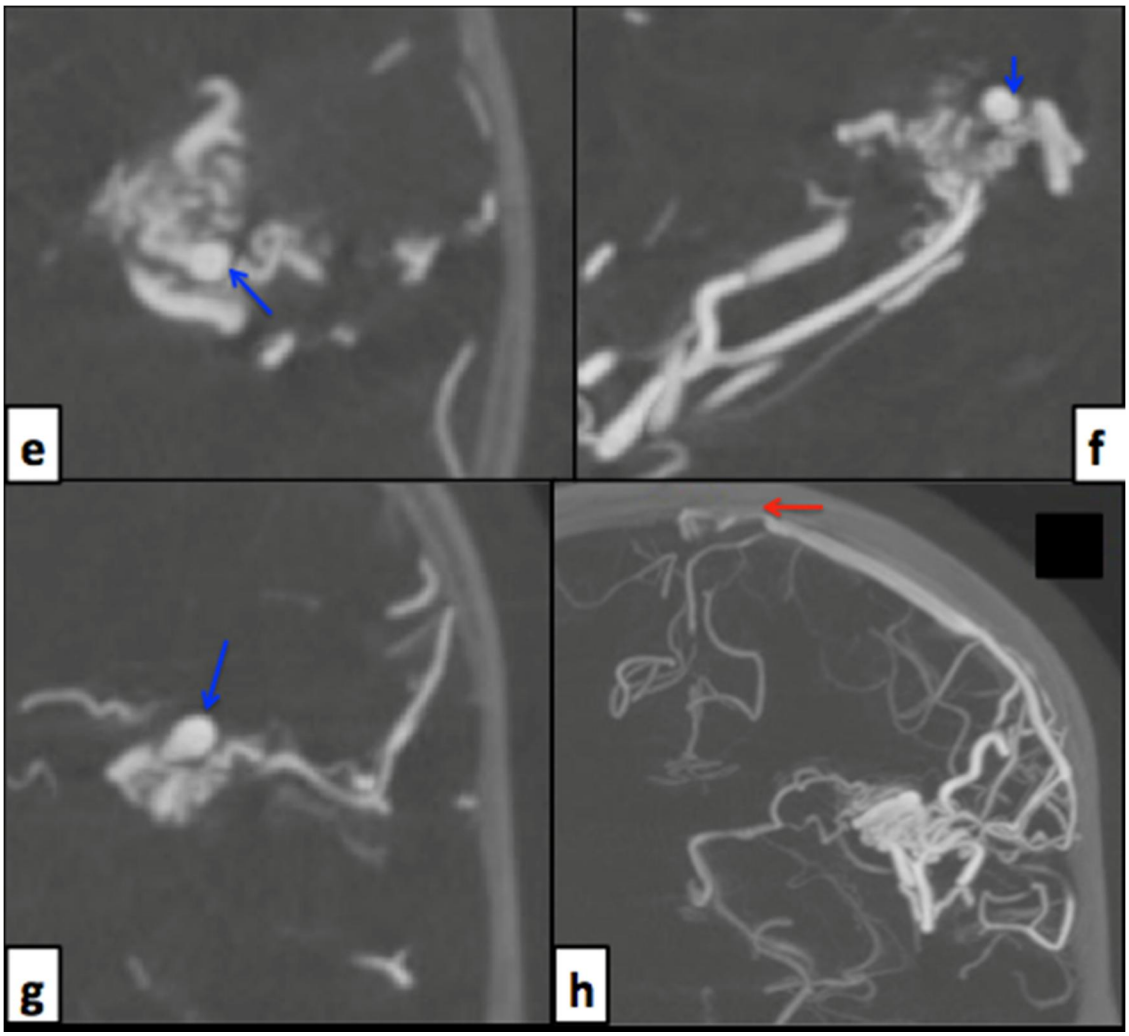

Multiplanar 3D RA images (e, axial; f, sagittal; g, coronal) more precisely demonstrating the morphological aspects of the aneurysm (blue arrow). h, Coronal 3D RA image showing the draining venous stenosis (red arrow).

Case 10.

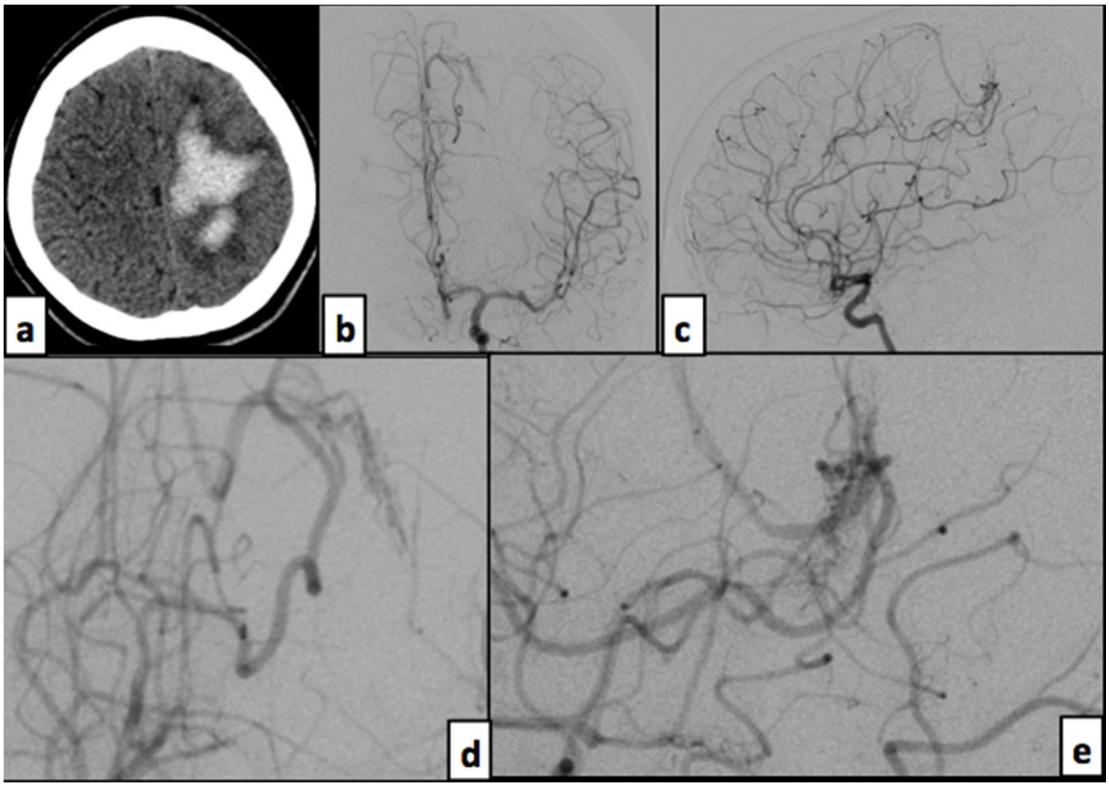

Ruptured AVM involving left paracentral lobule (a, NCCT head showing haemorrhage) with angiographic risk factors (b-e, left ICA angiographic images) of small size (maximum dimension of 9 mm) of the sparse nidus and exclusive single superficial draining vein.

Case 11.

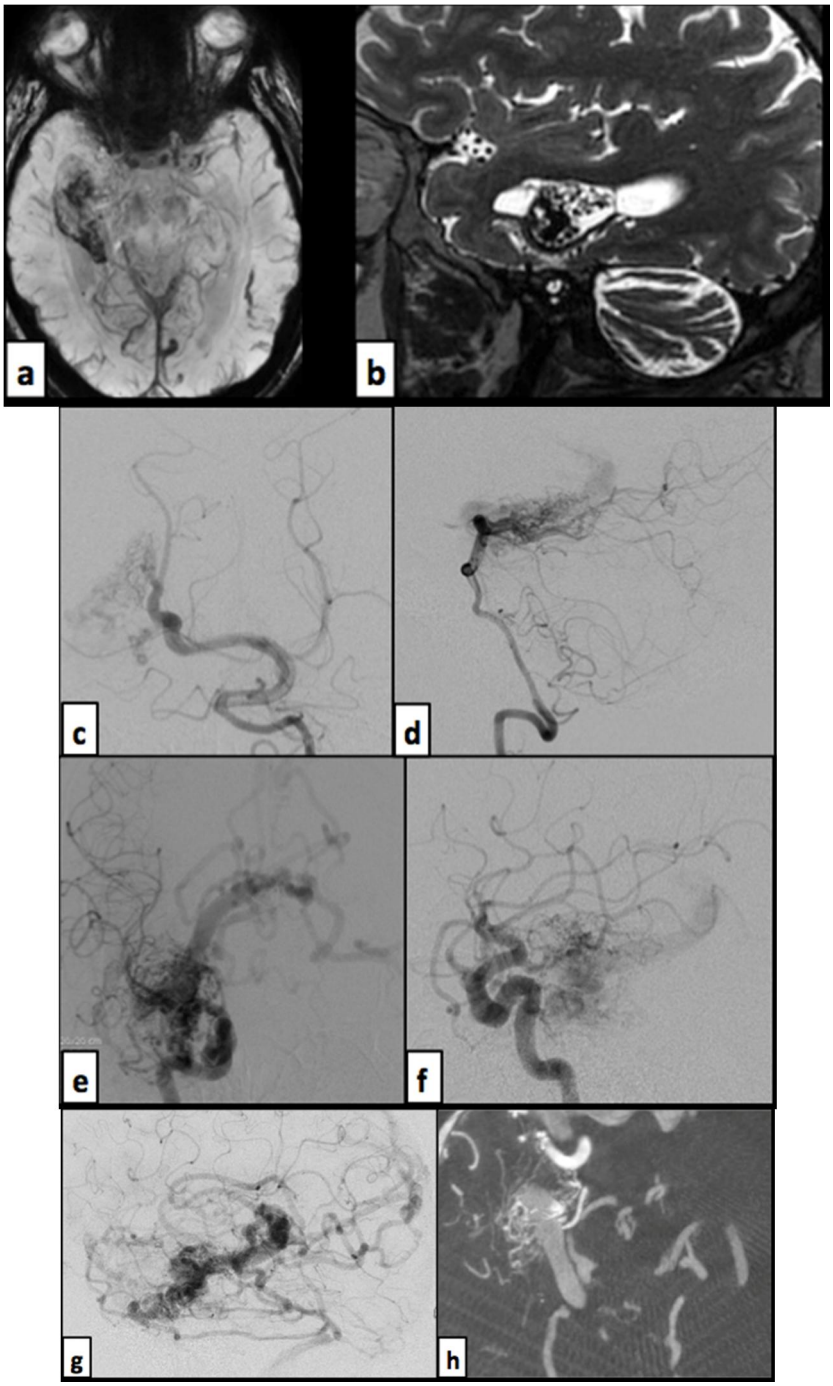

Hemorrhagic risk factors in BAVM of a 40 years old man: choroid plexus location (a, Susceptibility weighted MRI; b, Sagittal T2WI), choroidal feeders (c and d, left vertebral artery angiograms demonstrating the right posterolateral choroidal artery feeder; e and f, right ICA angiograms demonstrating multiple small feeders from the right anterior

choroidal artery) and single deep draining vein (basal vein of Rosenthal).

g, Venous phase of right ICA DSA (lateral view) revealed occlusion or aplasia of the straight sinus and consequent ipsilateral and transcerebral venous collateral rerouting (e, g).

h, Axial 3D RA image depicting the fistulous site of the AVM – direct communication of the right anterior choroidal artery branches into the anterior aspect of basal vein of Rosenthal. The difference in contrast intensity at the fistulous shunting zone is evident in the image.

Case 12.

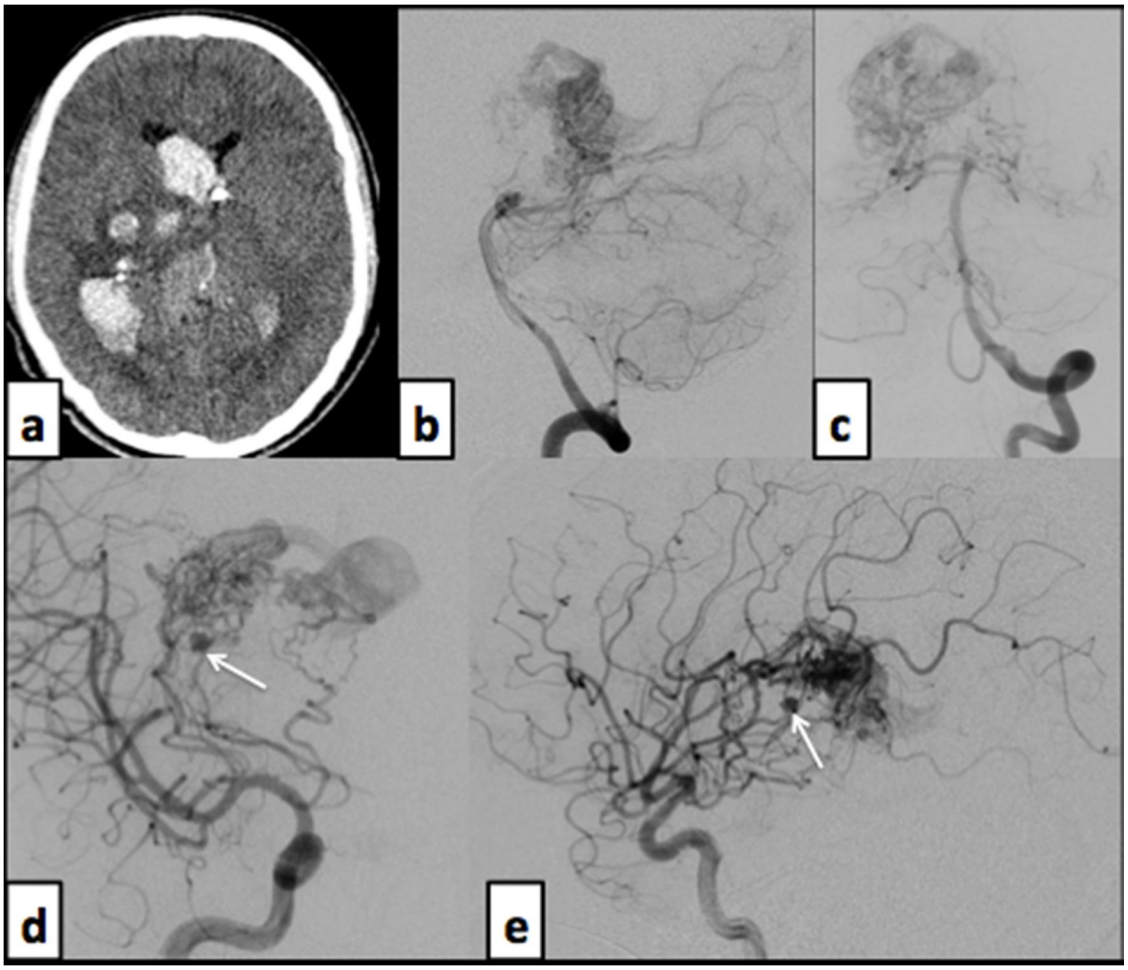

19 years old male patient presented with predominant right lateral ventricular and associated focal right thalamic – basal ganglionic haemorrhage (a, NCCT head). Angioarchitectural risk factors for haemorrhage in this AVM include: choroid plexus – thalamic - basal ganglion location, arterial feeders from posterior choroidal artery (b and c, left vertebral artery angiograms), lenticulostriate and anterior choroidal arteries (d and e, right ICA angiogram), a distal flow-related aneurysm (white arrow) in the lenticulostriate artery and exclusive single deep venous drainage.

Case 13.

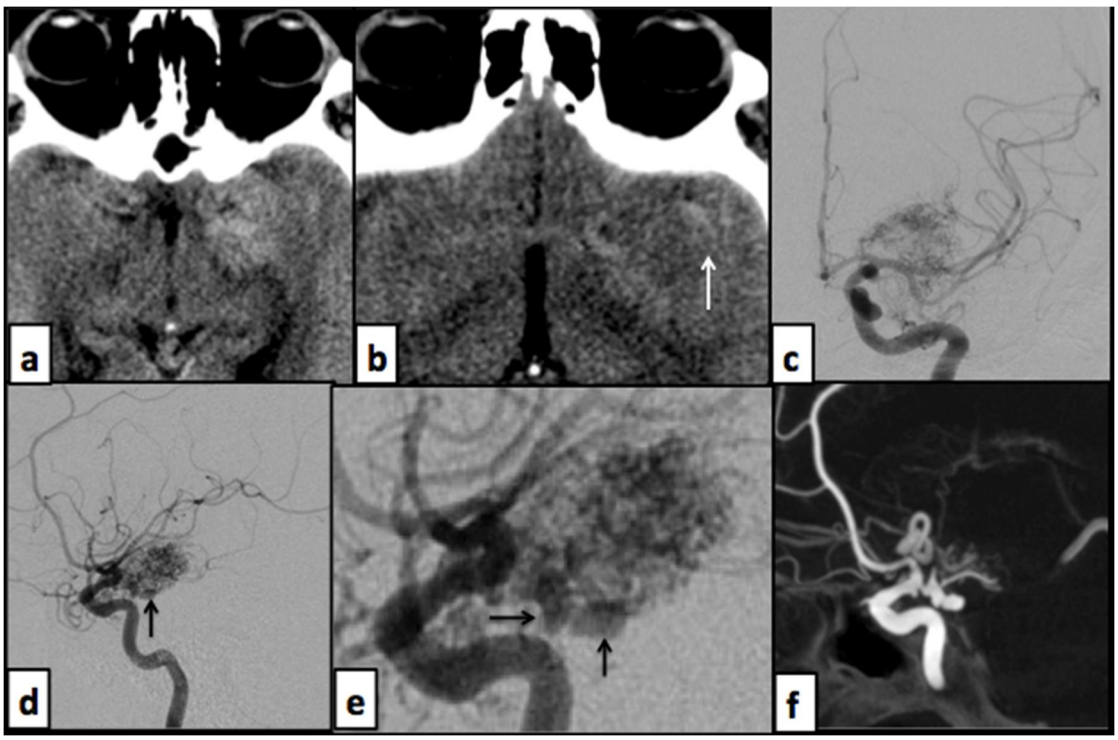

a and b, NCCT head of a 36 years old man who complained of acute onset headache, revealed left anteromedial temporal sulcal subarachnoid haemorrhage (white arrow). c, d and e, Left ICA DSA demonstrating left choroidal plexal compact nidus AVM and two distal flow-related aneurysms (black arrow). f, 3D RA sagittal reconstructed image depicting true morphology and origin of the proximal feeding artery aneurysm - a bilobed and narrow necked saccular aneurysm of proximal anterior choroidal artery. The location & morphology of the aneurysm correlates with the source of haemorrhage. Such vital information from 3D RA was decisive for apt therapeutic strategy of coiling of the aneurysm rather than embolization of the unruptured AVM as the initial management step.

Case 14.

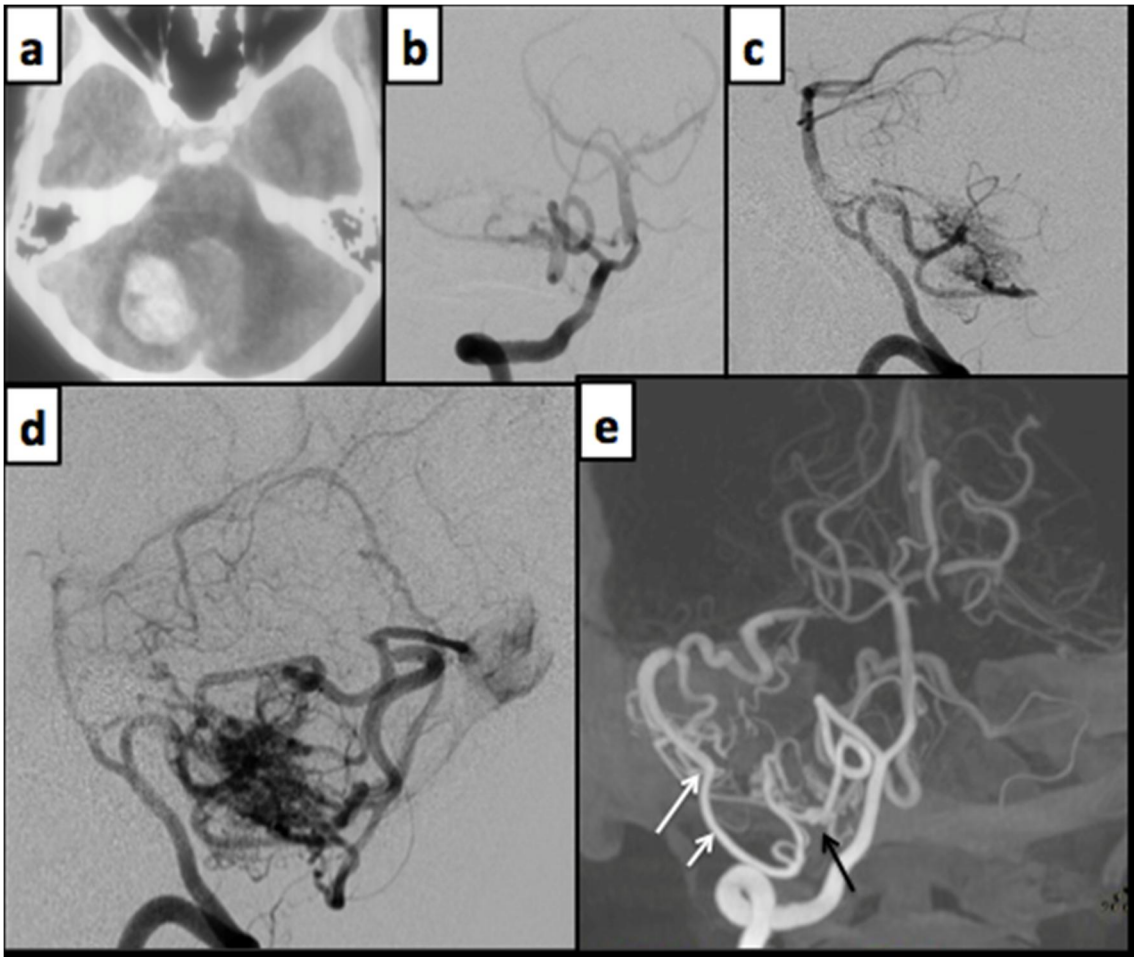

a, NCCT head showing right cerebellar haematoma in a 30 years old woman. Right vertebral artery angiographic images in early arterial phase (b and c) didn't demonstrate any aneurysm associated with the cerebellar AVM. Sequential DSA image (d) showing early draining veins within 0.5 seconds of the arterial phase onset, an indirect evidence of fistulous component in the nidus. e, 3D RA coronal MIP image demonstrating the distal flow-related aneurysm in right posterior inferior cerebellar artery (black arrow) and fistulous site (long white arrow) in the nidus (short white arrow – arterial feeder to the fistula).

Case 15.

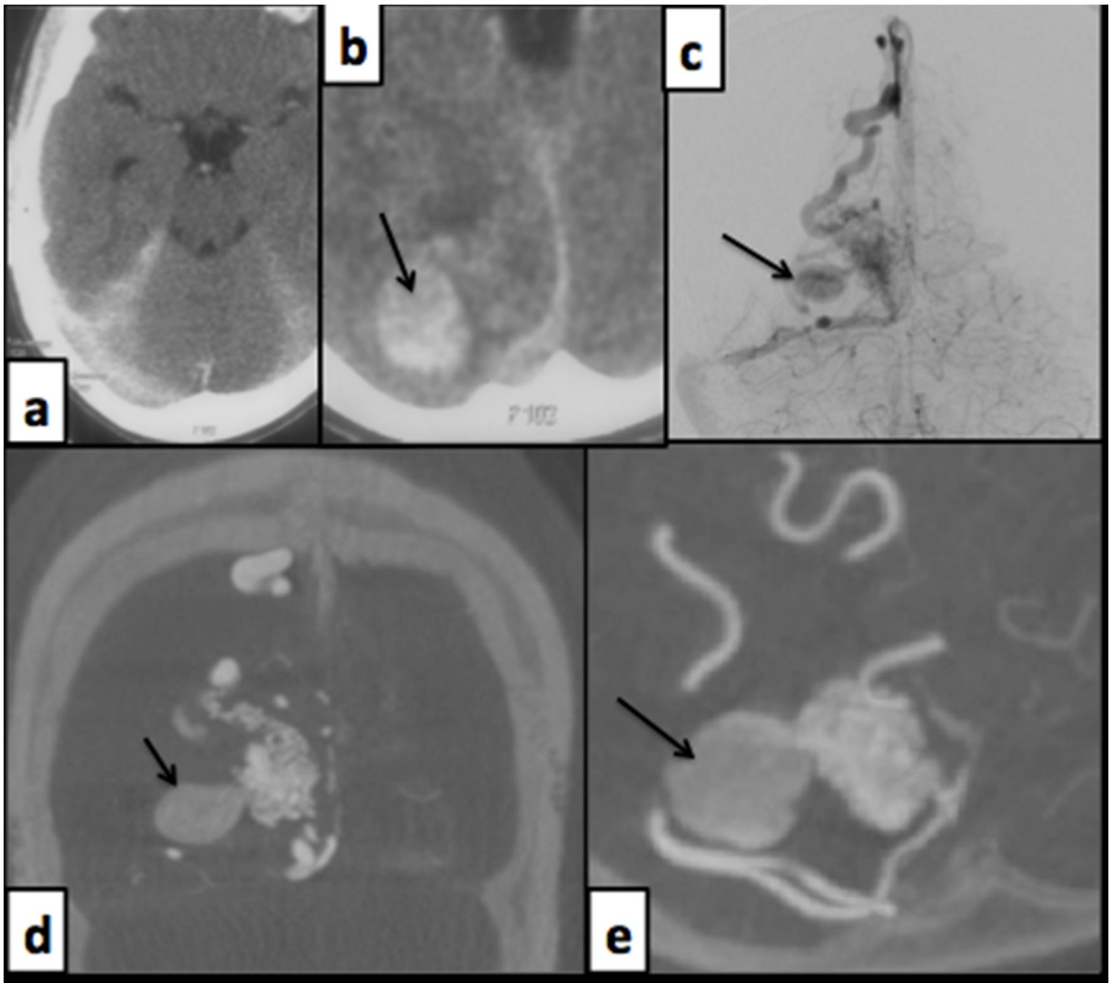

Tentorial subdural haematoma (a, NCCT head) in a 16 year old male patient with right occipital compact nidus AVM (c, vertebral artery angiogram; d and e, 3D RA coronal and axial images) was possibly caused by the rupture of perinidal venous pseudoaneurysm (black arrow). In an AVM, pseudoaneurysm forms as a result of rupture of the lesion and further, it acts as a potential source of rebleed.

B. Seizure

Case 16.

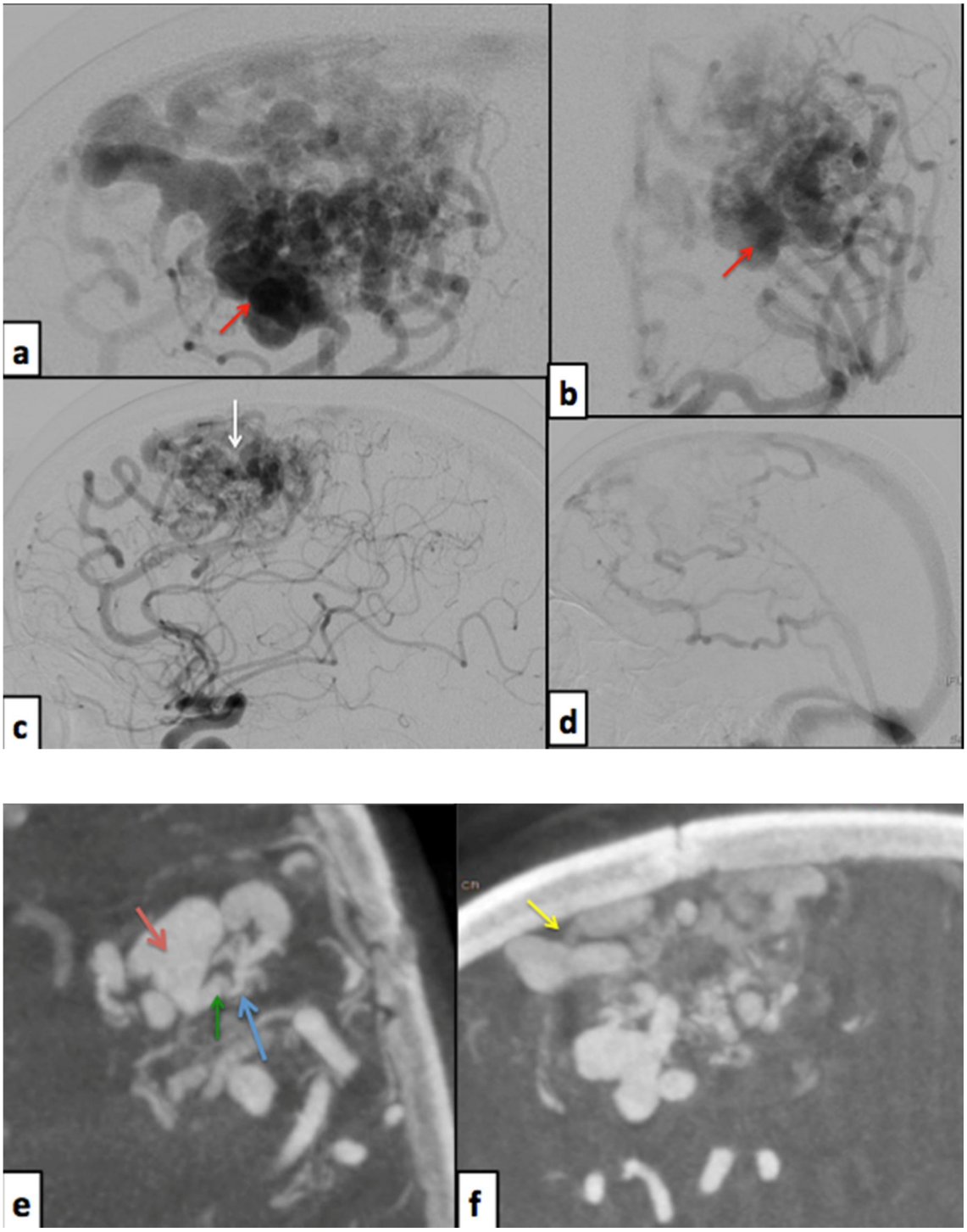

Angiographic predictors of seizure disorder in BAVM. a and b, Lateral and AP early arterial phase images of left ICA DSA demonstrating a

diffuse nidus left frontal AVM measuring 46 mm in maximum dimension, with indirect evidence of associated fistulous component (visualization of early draining veins in early arterial phase within 0.5 seconds of the arterial phase). Red arrow - intranidal venous varix. c, Right ICA DSA depicting perinidal angiogenesis (white arrow) from right ACA branches. d, Ipsilateral venous collateral rerouting. e and f, Advantages of 3D RA images depicting the exact fistulous site (blue arrow - feeding artery pedicle, green arrow - fistulous site and red arrow - venous varix) and the venous outflow stenosis (yellow arrow).

Case 17.

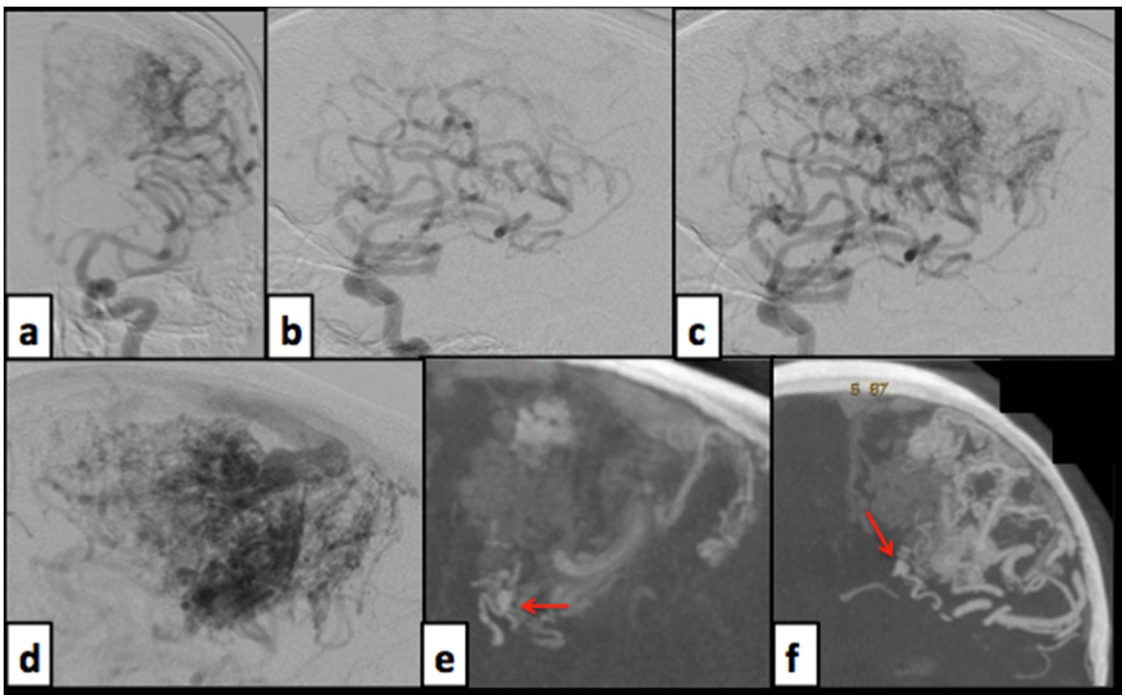

51year old man with seizure disorder. Left ICA selective angiography (a, anteroposterior projection; b, c, and d, sequential lateral images) demonstrating a large diffuse nidus AVM in left fronto-parietal lobe. No aneurysm was identified in the DSA images. 3D RA images (e, lateral and f, coronal) depicting a very small distal flow-related aneurysm in the unbled AVM.

C. Headache

Case 18.

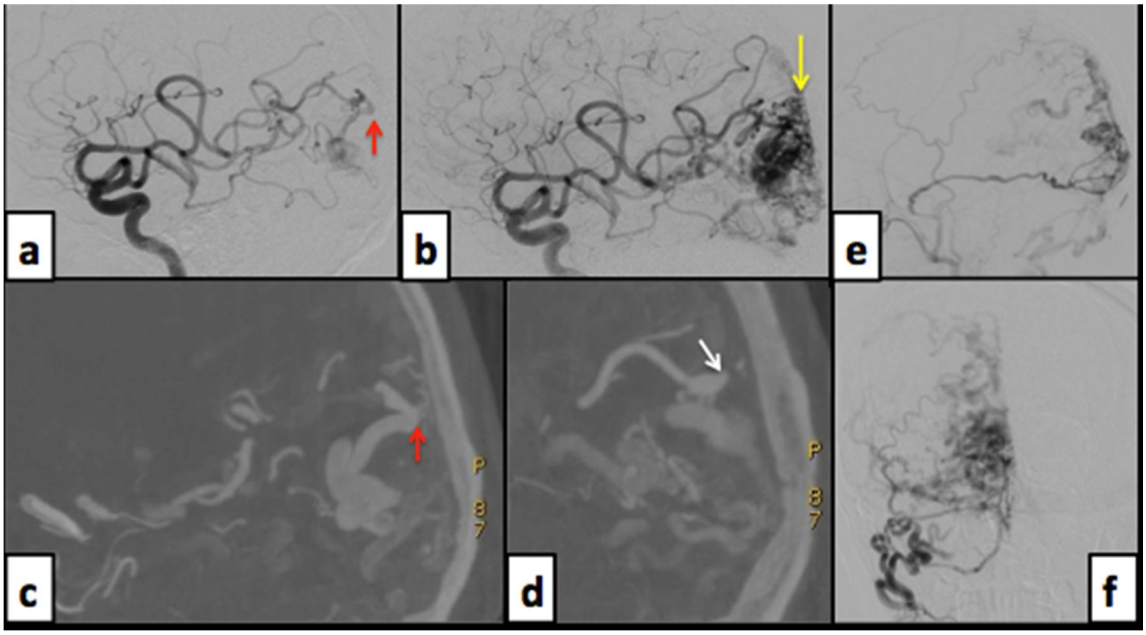

Unbled right occipital AVM in a 63 years old man with clinical presentation of chronic headache. Recruitment of dural feeders (e and f, lateral and anteroposterior images of right ECA angiogram demonstrating feeders from middle meningeal artery) and perinidal angiogenesis (yellow arrow in figure b) have significant increased association with headache.

a, Lateral projection of right ICA angiogram in early arterial phase and b, 3D RA lateral image depicting the direct continuation of the angular artery feeder into a dilated vein; fistulous site (red arrow) in the nidus. d, 3D RA image showing a small distal feeding artery aneurysm (white arrow). No aneurysms were visualized in the 2D DSA images.

Case 19.

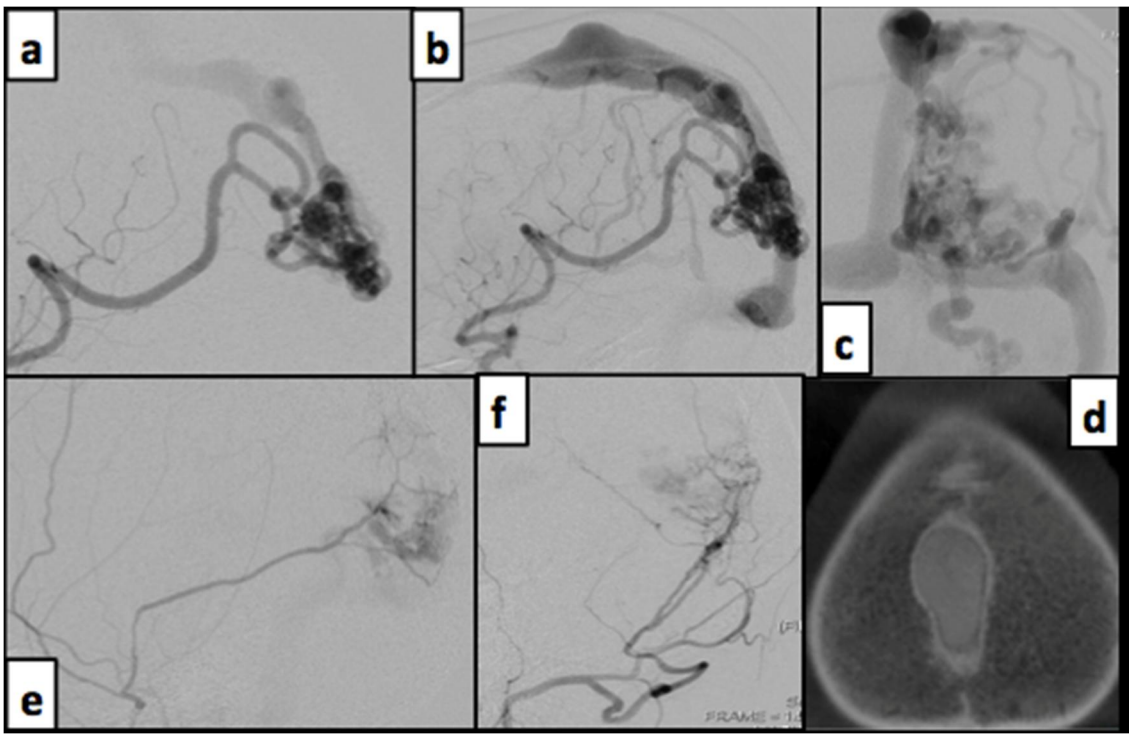

Left occipital unbled AVM in a 32 years old woman with clinical manifestation of chronic headache. a, Lateral projection of left ICA angiogram early arterial phase demonstrating visualization of early draining vein within 0.5 seconds, indicating presence of fistulous component. The fistula was not seen in the 3D RA. b and c, Lateral and anteroposterior images of left ICA DSA depicting an ectatic occipital cortical vein draining the AVM into superior sagittal sinus (SSS). Mid SSS focal ectasia is scalloping the calvarium (d, reconstructed axial image of 3D RA), likely cause of headache of this patient. e and f, Left ECA feeders (middle meningeal and occipital artery) to the AVM was also seen.

D. Neurological symptoms or deficits

Case 20.

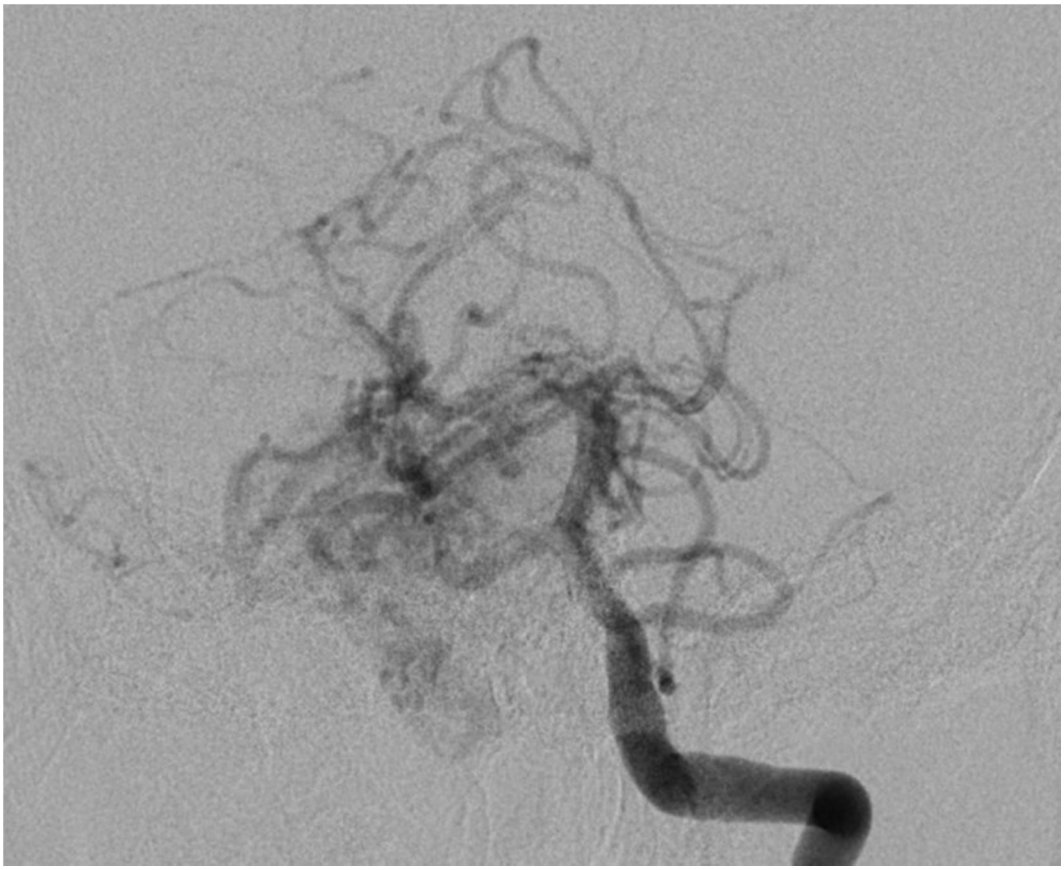

35 years old man presented with right-sided tinnitus. Left vertebral artery angiogram demonstrating a right cerebellar diffuse nidus AVM with arterial feeders from right anterior inferior and superior cerebellar arteries and multiple superficial hemispheric draining veins. Localised high flow shunt near the right internal auditory canal being the cause of the focal neuro-otologic symptom in the patient.

DISCUSSION

Introduction

According to the literature, 3D RA is used mostly for the assessment of cerebral aneurysms. As 3D RA can provide substantial additional information on BAVM, we routinely perform 3D RA for neuroangiographic evaluation of brain AVM for diagnostic purpose as well as for decisive management. 3D RA acquisition can eliminate multiple oblique angiography injections, thereby helping to decrease the overall contrast load used for angiographic explorations. Furthermore, the patient's radiation dose is reduced, as the 3D RA radiation dose is significantly lower than that of biplanar DSA.

Criteria and Definitions

The vascular composition and intrinsic angioarchitecture of the nidus cannot be evaluated adequately by selective internal carotid or vertebral angiography. Simultaneous visualization of different, haemodynamically independent compartments, overprojection of large venous structures on the nidus and flow related poor or non-visualization of various vascular elements limits precise nidus evaluation. 3D RA images are also stilted for detail interpretation due to poor temporal resolution. Superselective angiography of the individual feeding arteries delineates the architectural and composition mapping of the nidus and it is the usual gold standard for detecting fistulous components and intranidal vascular cavities. However superselective angiograms were obtained only in limited number of patients who underwent embolization in the same sitting.

Based on the experience obtained from routine application and systemic interpretation of superselective feeder injections performed before or during the course of embolization procedures of brain AVMs, new insights and concepts regarding the nidus of the AVM have been developed and progressively incorporated in the angiographic interpretation. Following criteria were used during interpretation of the images of DSA and / or 3D RA to define the particular entity as detailed below.

Nidus appearance: Three types of appearance of the nidus were determined independently by evaluating the DSA and 3D RA images.

a) Compact nidus: Close-packed arteriovenous shunting zone (nidus) with well defined borders and homogeneous appearance (as there is no intervening brain tissue).

b) Diffuse nidus: Diffuse appearance of the nidus involving a large lobar or multilobar area without clearly defined borders and does not have a compact and homogeneous appearance (as it contains intranidal cavities, normal brain tissue within). Perinidal angiogenesis is carefully excluded as part of the nidal definition, while interpreting the selective injections in DSA or 3D RA.

c) Sparse nidus: Localized thinly dispersed nidal network without any significant enlargement of the feeding artery and draining veins.

Intranidal aneurysm: Arterial intranidal aneurysms are visualized in early arterial phase of DSA. They are located on the nidal ramifications of the feeding arteries and should not be traceable to the draining vein, thus obviating possibility of venous sacs or aneurysms to be wrongly considered as intranidal aneurysm. Such arterial outpouchings of more

than 1 mm size are considered as aneurysms.

Suspicious intranidal vascular outpouchings observed in the later phase of DSA, thereby precise visualization hindered due to overlap of draining veins and nidal vessels, are considered as 'possible' intranidal aneurysms (in 2D DSA).

Fistulous component in AVM:

i) Observation of direct arteriovenous communication in DSA or 3D RA.

ii) Indirect evidence in DSA as visualization of early draining vein within 0.5 seconds of the visualization of arterial feeding pedicle or opacification of the early draining vein before visualization of the nidal network

iii) In 3D RA, if the distal segment of the feeding arterial pedicle could be traced into a single vascular channel from which the proximal segment of the draining vein is seen to emerge.

COMPARISON OF 3D RA WITH DSA

1. Flow related aneurysms

With the advent of 3D RA, the technique has been predominantly utilized for assessing the cerebral aneurysms.

Few comparative studies have been carried out in recent past between 2D and 3D DSA in evaluation of intracranial aneurysms. It has been shown that 3D DSA is more sensitive for depiction of intracranial aneurysms than is 2D DSA.

X. Combaz *et al.* compared DSA with 3D RA in 72 patients with brain AVM and reported significant higher detection of AVM associated aneurysms, specially the intranidal aneurysms with 3D RA *vs* DSA.[53]

Therefore, we have considered 3D RA as standard of initial neuroangiographic investigation for detecting any AVM associated flow related aneurysms. In the present series, 3D RA was more accurate and sensitive for detecting AVM associated flow related aneurysms as compared to DSA. DSA showed low sensitivity (43.1%) and specificity (73.4%) for detecting intranidal aneurysms. 3D RA also detected significantly higher number of AVM patients with feeding artery aneurysms as compared to DSA. Incidence of intranidal, perinidal and flow related feeding artery aneurysms in this series was 34.7%, 3.6% and 12.6% respectively.

Multiplanar postprocessed images of 3D RA are advantageous in detecting the aneurysms, which could be traced along the feeding artery ramification without any direct continuity to the venous channels. In DSA, overprojection of plexiform or fistulous nidal vessels and dilated early draining veins may obscure visualization of small feeding artery pedicles as well as small flow related aneurysms located within or in proximity to the nidus. In DSA, we have also obtained single plane images of the AVM with maximum frame rate of 7.5 per second. DSA images acquired with higher frame rates with high temporal resolution failed to detect these small aneurysms accurately. Early opacification of the homogeneous compact nidus poses further difficulty as compared to a sparse network of nidus in the biplane images of DSA.

Eleven intranidal (20%) and one perinidal (20%) aneurysms were wrongly considered as arterial site aneurysms in DSA; however 3D RA

images clearly depicted these outpouchings to be part of plexiform nidus or in direct continuity with the draining venous channels.

Small venous aneurysms or varices are precisely diagnosed from 3D RA by virtue of continuity of such outpouchings with the draining venous channels.

Both DSA and 3D RA demonstrated similar accuracy in visualizing large venous varices.

Only a few cases demonstrated intranidal pseudoaneurysms and these irregular shaped aneurysmal cavities could be identified both in DSA and 3D RA.

2. Arterial feeder

Dominant arterial feeders could be identified with accuracy in both DSA and 3D RA; in few cases distal course of the arterial feeder could be clearly depicted in 3D RA as against overlap of adjacent vessels in 2D DSA. Thus 3D RA is advantageous, specially while planning the endovascular intervention for optimal positioning of the image intensifier anticipating the projection that would give the best visualization of the origin of the branches, and allow the navigation and positioning of the microcatheter for injection of the contrast agent.

A precise mapping of the malformation could be obtained with identification of each feeding artery, as well as arteries at the border of the AVM, by combined analysis of the vessels of interest on anteroposterior and lateral views of the angiogram and the 3D RA.

3. Angiographic pattern of nidus

Good agreement was seen between 3D RA and DSA while interpreting the angiographic appearance of the AVM nidus as compact, diffuse or sparse as per the laid down criteria. In Few instances the nidus could be more well delineated in 3D RA.

As nonenhancing nonvascular space within the nidus could be discerned on 3D RA; it may be more accurate to infer about nonvascular nidal cavities. However MRI is the apt modality to identify intranidal gliosis, area of bleed or normal brain tissue.

As demonstrated in the present study that 3D RA is precise and superior to DSA for detecting intranidal vascular cavities comprised of arterial aneurysms, arterial loops, venous intranidal varices and has similar accuracy as DSA for detecting nidal pseudoaneurysms; thus true nidal appearance may be better delineated in 3D RA. However as the processed 3D RA images are static, ignoring critical dynamic informations of the DSA, especially superimposition of the veins obscuring the nidus detail, DSA has unique advantage for it's high temporal and spatial resolution. This could account for the observations in the present study, that there is no significant difference between DSA and 3D RA to classify the angiographic appearance of the nidus.

Combined analysis of multiplanar images of 3D RA and anteroposterior and lateral images of 2D DSA would elucidate the nidal architecture more precisely.

4. Fistulous component

Direct arteriovenous communications (fistulae) are evident in significantly higher number of 77 cases on 2D DSA images as compared to 52 cases detected from 3D RA. Only one case in which fistulous component could be visualized in 3D RA, remained undetected by DSA. However in DSA, fistulous component in the nidus was diagnosed mostly by means of indirect evidences as elaborated in the criteria to consider fistulous nidus. Second, only superselective angiogram could elucidate the definitive fistulous components; but superselective microcatheter angiogram was obtained in a very few patients in this study at same sitting and the observations from DSA or 3D RA were not compared with this gold standard.

As fistulous arteriovenous shunts are diagnosed in 3D RA by observing the direct communication between feeding arterial pedicle with the draining venous channel; accuracy of 3D RA for detecting the fistula is proposed to be high. 3D RA depicts the arterial feeder to the fistula in explicit manner, thus helpful in determining the target arterial feeder for embolization of the high flow shunt component.

5. Draining vein stenosis

Significantly higher number of cases with draining vein stenosis was detected with 3D RA (21.6%) *vs* DSA (13.2%) ($P < 0.001$). To specifically detect stenosis of the draining veins or sinuses and hypoplasia or aplasia of the venous sinuses, DSA images have to be obtained along the profile of the venous channel course. With rapid transit time across the AVM lesion; acquisition of 3D RA images in five to seven seconds time frame allow visualization of primary draining veins. Multiplanar postprocessed images of 3D RA are advantageous to depict the venous

channels with stenosis.

6. Venous drainage and other venous high-flow angiopathy

The anatomic type of veins draining an AVM can usually be predicted from the location of the lesion. It is well documented in literature, that in up to 30% of cases, an unexpected venous drainage pattern is observed angiographically for both superficial and deep brain AVM.

Selective angiography is needed for evaluation of the AVM draining veins. It is also essential in providing information on the venous drainage of normal brain parenchyma and its relation to the draining veins of AVM.

3D RA static images are limited by overlap of the normal parenchymal draining venous phase and therefore, may not be able to distinguish between venous collateral rerouting and venous egress from normal brain. Apart from delineating the course and number of main draining veins and stenosis in its course or near the junction with venous sinus and stenosis in the draining venous sinus, 3D RA has limited role in assessing the venous drainage of the AVM. Also, with five seconds of tube rotation time to acquire the 3D RA images, venous egress from normal brain parenchyma contaminates the static image of 3D RA.

Therefore, primary venous drainage of AVM or the collateral venous rerouting and normal brain parenchymal venous egress patterns and cerebral circulation time could be analysed primarily from the dynamic DSA images.

With multiple exit veins or extensive venous collateralization, 3D RA images may complement the interpretation of DSA images for venous drainage pattern amidst overlap of multiple veins.

CORRELATION OF ANGIOARCHITECTURE WITH CLINICAL PRESENTATIONS OF BAVM

1. Haemorrhage

Haemorrhage was the most common presenting symptoms (98 cases, 58.7%) in this study, similar to the trend observed in literature, haemorrhage being reported to occur as the initial manifestation of the disease in approximately 50% of patients with an AVM.

Several studies have correlated the angiographic features with the clinical presentation of haemorrhage in patients with brain AVM. Our analysis yielded smaller AVM size, deep supratentorial location, infratentorial location, single draining vein, sparse or compact nidus and small perforator or choroidal arterial feeders as being significantly associated with initial haemorrhagic presentation. However we didn't find any strong statistically significant association with distal flow related aneurysms, stenosis or occlusion of draining veins and venous varices.

Smaller AVM size

Several studies have shown that small AVMs (< 3 cm) are at higher risk of haemorrhage. Conversely studies of Berenstein at al, Marks et al, Ondra et al suggest, that there is no direct correlation between the size of the AVM and the incidence of haemorrhage. In the present study, we found significantly high rate of haemorrhagic presentation between small AVMs (67.7%) compared with larger AVMs (46.5%).

The underlying pathophysiology for such association remain uncertain. It has been postulated, that small and micro-AVMs are at higher risk of haemorrhage than larger AVMs because the pressure in the arterial feeders and the nidi were found to be significantly higher than in

larger AVMs.[68] This notion could also explain disproportionately larger haematoma sizes in smaller AVMs.

Location of AVM and arterial feeders

Several studies have shown that deep parenchymal and infratentorial location of AVM pose increased risk of haemorrhage. In the present study incidence of haemorrhage was significantly higher in deep or central brain AVM (85.7%), insula-opercular region (70%) and infratentorial location (66.7%).

We have analysed that brain AVMs with predominantly lenticulostriate or small perforator and choroidal arterial feeders were more likely to present with haemorrhage (92% cases). Also these arteries are the usual feeders to the deep brain AVM. These small perforator arteries lack adequate mural support and are thin in caliber; thus more prone for rupture under higher pressure due to arteriovenous shunting.

Although comprising only 7 to 15% of intracranial AVMs, hemorrhage rates of infratentorial AVMs among adult surgical series range from 72% to 92%, and studies have identified infratentorial location as independently associated with both initial and future AVM hemorrhage. This high hemorrhage rate has been explained by several factors, including the high frequency of perforator supply and exclusive deep venous drainage, as well as ‘kinking’ of the venous system at the level of the tentorium. Because infratentorial AVMs are less likely to present with seizures, some authors have suggested that this may contribute to the higher rates of hemorrhage observed among reported series. Infratentorial AVMs are usually associated with increased incidence of distal feeding artery and nidal aneurysms. These aneurysms are considered as vascular weak points for bleed. Also haemorrhage

associated with infratentorial AVM manifests with early and aggressive clinical course.

Subtle bleed in the eloquent deep parenchymal location involving basal ganglion, thalamus, hypothalamus, internal capsule generally causes more severe neurological symptoms than does bleeding from lesions located in the superficial brain parenchyma. Therefore minor haemorrhage in superficial brain location may remain undetected, which could partly account for the increased detection of deep parenchymal bled AVM. Small chronic haemorrhagic areas are observed on MRI or during microsurgical removal of superficial brain AVMs in patients, in whom these events have not been detected clinically.

Single draining vein

In our series single draining superficial or deep vein was associated with significantly higher risk of haemorrhagic presentation in brain AVM.

Daniel *et al.* in a cohort of one hundred and twenty two patients with brain AVM, showed that single draining veins were at increased risk of rupture because of increased outflow impedance. A very high association of exclusively deep venous drainage was demonstrated with single draining venous disposition, which increased the haemorrhage risk.[3]

Marks *et al.* found hemorrhagic presentation more frequently in patients with central venous drainage (94%) over cortical (37%) or mixed drainage (50%). Miyasaka *et al.* found a similar relationship, with 94% of AVMs with exclusive deep drainage presenting with hemorrhage. Because deep-seated AVMs are more likely to have a component of deep

venous drainage, previous studies have pointed out that the relationship between deep venous drainage and hemorrhage may be influenced by AVM location. Although one study identified deep location and not deep venous drainage as a significant factor at presentation, others have identified both deep drainage and exclusive deep drainage as independent predictors of hemorrhagic presentation. Prospective studies have also identified deep venous drainage and exclusive deep venous drainage as important risk factors for future AVM hemorrhage.

Nidus pattern

The results presented in this study provide empirical evidence supporting statistically significant differences amongst angiographic nidus pattern and clinical presentation of haemorrhage. To the best of our knowledge, this study is the first to test the correlation of nidal pattern to predict haemorrhage risk. Sparse and compact nidus was associated with high incidence of haemorrhage in brain AVM (85% and 60% respectively) as compared to diffuse nidus pattern (incidence of haemorrhage in 32% of cases) and sparse nidus was found to be a statistically significant predictor of haemorrhage ($P < 0.001$).

High arterial pressure could be responsible for rupture of the thin nidal vessels in case of sparse nidus. Conversely, in absence of nidal aneurysm, a sparse nidus would expect to demonstrate comparatively low flow shunt and lower pressure gradient across the nidus; thereby pose low risk for haemorrhage. Also an event of haemorrhage may alter the angiographic appearance of the nidus. Mass effect, gliosis or haemic cavity would disrupt the usual compact appearance of the nidus. An overall high incidence of sparse nidus (28% cases) being reported in the present study, could buttress the notion of alteration in nidal architecture

due to bleed. Further angiographic studies before and after the event of haemorrhage could elucidate this enigmatic nidal pattern.

Distal flow related aneurysms

Though higher number of patients of brain AVM with associated intranidal, perinidal or feeding artery aneurysms had haemorrhagic manifestation (63%, 67% and 57% cases respectively); the chi square test revealed no statistically significant correlations.

Similar to our observations, all the studies have reported higher incidence of flow-related aneurysms in bled AVM vs unbled AVM patients.

Most of the reports in literature indicate statistically significant association of aneurysms with haemorrhage. In the earlier studies of Marks *et al*, and Turjman *et al*, the association of intranidal aneurysms and haemorrhage has been found in 41% to 80% patients. This association was even stronger in the presence of multiple aneurysms. Turjman *et al,* have found intranidal aneurysms in 42% and multiple flow related aneurysms in 57% of patients; based on superselective angiographic evaluation of brain AVM.[62]

A number of studies have failed to demonstrate statistically significant association of aneurysms with haemorrhagic presentations in brain AVM. In a prospective study of 340 patients with brain AVM, univariate analysis revealed presence of aneurysm was not an independent predictor. Pollock et al also could not identify any relation between aneurysms and hemorrhagic presentation in a series of 313 patients.[69] Stefani et al found the occurrence of hemorrhage in 38 (50%) of 75 patients with intranidal aneurysms, however, multivariate

analyses in this group of patients failed to demonstrate any significant association with hemorrhagic presentation.[70] Daniel et al in a cohort of 122 patients with brain AVM, reported 66% incidence of associated aneurysms with presence of aneurysms in 74% of bled and 60% of unbled AVM cases. Though there was a trend toward significance for any associated aneurysms and haemorrhage was noted in their study (*P* value of 0.08 in univariate analysis); statistically the association was not strong.[3] In a recent study with a cohort of 135 patients of children and teenagers, Michael et al reported 11 (8%) children with associated aneurysms (seven patients with intranidal, four patients with proximal flow related aneurysms), nine (81.8%) of whom presented with hemorrhage. Despite this high rate of hemorrhage, this feature was not significantly associated even on univariate analysis, likely due to the small number of children with associated aneurysms.[63] However in our study, higher number of patients (34.7%) had associated intranidal aneurysms, yet we didn't find any significant association with haemorrhage.

We have contemplated few factors, which could elucidate such uncustomary result. First, incidence of flow related arterial aneurysms associated with adult AVMs varies in the literature and is complicated by inconsistent definitions and variations in imaging techniques. Most of the prior, especially the earlier studies, implicating nidal aneurysms as an independent predictor of haemorrhage in brain AVM have reviewed the DSA images alone to identify the aneurysms. Reported rates of intranidal aneurysm identification in association with AVMs have increased due to improvement in diagnostic techniques, particularly 3D.[53,71] 3D RA images being highly sensitive to detect AVM associated intranidal and perinidal aneurysms, significantly increased number (100) of such

aneurysms have been detected in the present study as compared to 2D DSA images (50). As we have considered 3D RA as gold standard for detection of aneurysms, small benign aneurysms have been detected in increased number among unbled AVM cases. Second, we haven't compared or analysed the size of the arterial aneurysms in DSA and 3D RA images. It was observed during the interpretation of the DSA images, that prominent nidal or perinidal aneurysms located on the proximal ramifications of the feeding arteries could be easily detected. However 3D RA could precisely detect very small aneurysms in the nidus and these aneurysms were hard to find conclusively in DSA images, especially in diffuse or compact plexiform nidi. Third, amongst the bled AVM patients, aneurysm alone may not be the cause or source of bleed. In a recent study aimed at identifying the source of bleed in brain AVM, the source of hemorrhage was identified in 44% cases (18 of 41 subjects) with flow-related aneurysms as the source in only seven cases (17%).[85] Fourth, pathophysiological postulation of severe venous hypertension may cause retrograde propagation of increased pressure towards the arterial side of the nidus and lead to rupture of intranidal arterial aneurysms. Therefore AVM associated aneurysm may be one of multifactorial determinant than an independent predictor of haemorrhage.

Nevertheless, AVM associated distal flow-related aneurysms represent a weak angioarchitectural element and a risk factor for AVM rupture. Because intranidal aneurysms have a thinner and weaker wall than the other arterial elements of the AVM, they represent the most likely site of rupture following intraarterial pressure rise, particularly if it occurs suddenly. Following embolization of a nidus compartment, a sudden increase in intraartrial pressure involving the non-occluded arteries supplying the remaining AVM may occur, predisposing

unprotected intranidal aneurysms to rupture. Therefore, it has been recommended that, embolization of AVMs should be first performed through feeding arteries either carrying flow related aneurysms or supplying compartments containing intranidal arterial aneurysms.[62] Few studies have also shown reduction in the rate of rebleed in brain AVM patients, who have undergone partial target embolization of the nidal aneurysms.

Negative correlation with venous collateral rerouting

One of the novel observations of this study was statistically significant negative correlation of bled AVM with the presence of collateral rerouting of the main draining veins.

Such collateral venous outflow develops as to mitigate the high proximal draining venous pressure in very high flow shunts or distal venous obstructions. Sufficient venous collateralization decreases the risk of rupture and prevents the development of neurological symptoms. AVM rupture caused by venous hypertension may occur at the venous side of the nidus, veno-nidal junction or rupture of intranidal or distal extranidal arterial aneurysms due to retrograde propagation of the increased pressure. Therefore angiographically demonstrated redistribution of venous flow in the ipsilateral, contralateral or transcerebral veins without evidence of venous congestion of the brain and by the absence of significant venous varix formation proximal to any obstruction connotes lower risk for haemorrhage.

No independent association with venous stenosis or venous varices

Venous stenosis or presence of venous varix was not associated with haemorrhagic risk in the analysis of our study.

Several AVM features that either promote or reflect the development of venous outflow restriction and subsequent disruption of the transmural pressure gradient across AVMs have been studied. Studies have noted higher rates of hemorrhage among AVMs with deep venous drainage obstruction, draining vein stenosis, a small number of draining veins and venous varices. However, other than single draining vein and exclusive deep venous drainage, no individual feature of the venous system was found to be significant on multivariate analysis in these studies.

2. Seizure

Seizures were the second most frequent presenting symptom of cerebral AVMs following haemorrhage, reported in 25% of patients in the present study. We have excluded any previous haemorrhage related gliosis evident on CT or MRI.

Diffuse nidus, size larger than 3 cm, presence of fistulous component, perinidal angiopathy, venous collateral rerouting were identified as risk factors for clinical manifestation of seizure in unbled AVM in this study.

Hypoxemia in the epileptogenic regions of brain is the underlying cause of seizures in AVM.

Location

Highest incidence of seizure was seen in AVMs involving frontal lobe (45.2%) followed by parietal lobe (38%), temporal lobe (23.8%) and

occipital lobe (19%). Multilobar involvement was seen in 23.8% of cases. AVMs located exclusively in nonepileptogenic area like basal ganglion, thalamus, choroidal plexus, cerebellum and brainstem didn't manifest as seizure disorder in the present series. AVMs with seizure manifestations demonstrated significant negative correlation with these deep brain & infratentorial locations and also with presence of predominant arterial feeders as lenticulostriate or small perforators and choroidal arteries.

In a cohort of 33 brain AVM patients with seizures and 45 patients without seizures, the frontal, temporal, and parietal locations of the BAVMs were significantly associated with the occurrence of seizures with an odds ratio of 5. Individual analyses for every single lobe and for different permutations of lobes (frontal and temporal, temporal and parietal, and so forth) were also performed in that study; however, these did not demonstrate any association. [73]

Larger size and diffuse nidus

Mean maximum diameter of cerebral AVMs manifesting with seizures was significantly larger in the present study.

Other studies have also shown that medium and large nidus sizes (3 – 6 cm and > 6 cm, respectively) were positively correlated with seizure occurrence, whereas small nidus size (< 3 cm) was negatively correlated with presentations with seizures.

A large AVM may be more likely to present with seizures because the overall 'sump effect' may be more prominent. Chronic vascular steal by AVMs may cause hypoperfusion-induced remodeling of the perinidal cortex, thus facilitating an epileptogenic milieu. Also large AVMs may have increased association with seizure disorder secondary to venous

congestion, induction of hypoxia-mediated signaling pathways, and propensity to cause pathogenic alterations in neuronal and glial components of the perinidal cortex. Fiestra *et al.* reported, using a combination blood oxygen level-dependent MRI and angiography, that impaired cerebrovascular reactivity and venous congestion, rather than arterial steal, correlated significantly with AVM-associated epilepsy. Seizure occurrence may also be related to the larger volume of tissue in the circumferential vicinity of the AVM, with a higher likelihood of affecting a potentially ictogenic zone, or it may be due to a more widespread hypoxemia. Holohemispheric brain AVMs (so-called cerebral proliferative angiopathy) typically present with seizures. Perfusion studies performed in patients with cerebral proliferative angiopathy were able to demonstrate a widespread hypoperfusion distant from affected brain tissue, indicating hypoxemia in apparantly healthy adjacent brain tissue.

In this study, diffuse appearance of nidus was significantly associated with seizure disorders in brain AVM (P=0.001).

Larger AVMs are usually associated with multiple dominant pial arterial feeders with increased risk of intranidal and perinidal gliotic ischaemic changes with resultant ill defined diffuse appearance of nidus and intranidal nonvascular cavities.

Fistulous component and perinidal angiogenesis

Results (both univariate and multivariate analyses) from our study revealed presence of fistulous component and perinidal angiogenesis was significant angioarchitectural predictors for clinical presentation of seizures in brain AVM. Both of these arterial features imply very high flow nature of the shunt with hypoxemia of perinidal tissue and

intervening brain parenchyma if any within the nidus.

In a study of cerebral AVM with seizures by J.J.S. Shankar et al, three arterial features (fistulous component, arterial dilation, and perinidal angiogenesis) were evaluated and of these the presence of a fistulous component had the strongest association with seizure occurrence.[65]

Venous features

Of the investigated venous features (number of draining veins, venous out-flow stenosis, venous collateral rerouting and venous varix), venous collateral rerouting or veno-venous reflux had significant association with seizure occurrence (P= 0.001).

Venous collateral rerouting and veno-venous reflux is induced by proximal venous hyper-pressure due to venous out-flow obstruction or very high flow shunting. Venous collateralization or veno-venous reflux decreases the risk of rupture, however, may cause congestion of adjacent pial veins destined to drain the normal parenchyma in vicinity, and thence causes seizures, cognitive decline or progressive neurologic deficits.

Another study have reported high odds ratio for venous stenosis and long pial course of draining vein with venous congestion due to functional or anatomical outflow obstruction as the underlying cause for seizure or cognitive decline.[65]

3. Headache

Chronic headache as the initial clinical presentation in brain AVM has been seen in 8.4% of cases in our study. Presence of dural arterial feeders to the AVM, perinidal angiogenesis and higher SM grade (grade 3 to 5) were significantly associated with AVM related headache.

In 1940, Ray and Wolff made clear from their experimental studies in headache that there were pain-sensitive and insensitive structures. The insensitive structures are the skull, choroid plexus, brain parenchyma, pial veins, pia arachnoid, and the ependymal lining of the ventricles. Stimulation of the scalp and galea produced localized pain at the site of stimulation. Stimulation of the large arteries produced exquisite pain sensitivity that was more pronounced the more proximal the stimulus.

Arterial stimulation led to pain in the temporal, retro-orbital, and frontal regions.

From the literature of proposed mechanisms of brain tumour headache, it could be postulated that headache comes from dural and blood vessel stimulation. Traction on pain sensitive dura and larger arteries due to raised intracranial pressure could be the cause of headache. However, we have observed prolonged circulation time and angiographic features of raised ICP in only one patient with headache and most of the patients with prolonged circulation time in this study manifested with seizures. Also, we didn't evaluate all the aspects of raised intracranial pressure in this study.

Innervation of the dura of middle fossa and middle meningeal vessels is through trigeminal nerve. Cortical spreading depression may lead to headache via alterations within the meningeal vessels and resulting activation of the trigeminovascular system. Hypertrophy and high flow observed in middle meningeal arterial feeders to the AVM in this study may trigger the trigeminovascular system to cause headache.

The observed association of perinidal angiogenesis in this study was appurtenant to the postulation that, steal phenomena from the high-flow arteriovenous shunting in AVM may lead to headache.

Existing literature on BAVM associated headache mentioned about, occipital lobar location or posterior cerebral arterial feeder predominance being associated with symptoms of headache . However we didn't observe any such association.

4. Neurological symptoms or deficits in unbled AVM

Besides seizure and headache, neurological symptoms in unbled AVMs are rare, observed in nine patients (5.4%).

Observed location based symptoms in the study include difficulty in speech, gait ataxia and incoordination in cerebellar AVM and contralateral mild hemiparesis and paraesthesia in thalamic AVM. However, vast majority of the unbled cerebral AVM patients were asymptomatic for the location based expected deficits, supportive of the hypothesis that AVM being an incipient congenital lesion which evolves and manifests in young adults, thence the lesion is in equipoise with brain parenchyma and plasticity of functional brain area prevents focal deficits. Therefore localized symptoms could be triggered by altered haemodynamics and associated with vascular steal phenomenon, localized mass effects, venous hypertension, focal gliosis or chronic microhaemorrhage.

One patient with right cerebellar AVM developed right-sided tinnitus, attributed to hypertrophic shunting vessels near right internal auditory canal.

Proptosis of left eye was observed in one patient with parietal AVM with venous rerouting into the left cavernous sinus and retrograde flow into left superior orbital vein.

Cognitive decline was observed in one patient with AVM associated draining vein and sinus thrombosis.

LIMITATIONS

1. Observational bias (Detection bias) as interpretation of the 3D RA was carried out with the knowledge of the 2D DSA images, however 2D DSA was not taken as reference standard and secondly, all the observed variables were clearly defined.

2. Absence of superselective angiography in all cases.

3. Acute or subacute haematoma related altered angiographic appearance of nidus.

4. Assessment of multilobar brain AVM was limited as 3D RA was obtained depicting the main dominant feeder and vascular territories with lesser degree of contribution was not assessed by 3D RA.

CONCLUSION

3D RA is better than 2D DSA for detecting BAVM associated distal flow related aneurysms and draining venous stenosis. Also, 3D RA precisely depicts the dominant feeding artery course and the site of AV fistula in the nidus. 3D RA significantly improves the characterization of the brain AVM, necessary for planning the treatment strategy.

Incorporating 3D RA with DSA, in this cohort of 167 patients, smaller AVM size, single draining vein, deep brain and infratentorial location and predominant choroidal or perforator arterial feeders were associated with haemorrhagic presentation. Larger size, diffuse nidus, fistulous component, venous collateral rerouting and perinidal angiogenesis were the predictors of seizures in unbled BAVM. Recruitment of dural arterial feeders, presence of perinidal angiogenesis and higher SM grade BAVMs were associated with symptoms of headache. Involvement of eloquent locations were found to be associated with focal neurological deficit or symptoms in unbled AVM.

REFERENCES

1. Heidenreich JO, Schilling a M, Unterharnscheidt F, et al. Assessment of 3D-TOF-MRA at 3.0 Tesla in the characterization of the angioarchitecture of cerebral arteriovenous malformations: a preliminary study. Acta radiol. 2007;48(6):678–86.

2. Atkinson RP, Awad IA, Batjer HH, Dowd CF, Furlan A, Giannotta SL, et al. Reporting terminology for brain arteriovenous malformation clinical and radiographic features for use in clinical trials. Stroke. 2001;32(6):1430–42.

3. Sahlein DH, Mora P, Becske T, Huang P, Jafar JJ, Connolly ES, et al. Features predictive of brain arteriovenous malformation hemorrhage: Extrapolation to a physiologic model. Stroke. 2014;45(7):1964–70.

4. Da Costa L, Wallace MC, Ter Brugge KG, et al.The natural history and predictive features of hemorrhage from brain arteriovenous malformations.Stroke. 2009;40(1):100–5.

5. J. Moret, R. Kemkers, J. Op de Beek, R. Koppe, E. Klotz, and M. Grass. 3D rotational angiography: clinical value in endovascular treatment: Medica Mundi. 1998;42(3): 8 -14.

6. Ishihara S, Ross IB, Piotin M, Weill A, Aerts H, Moret J. 3D Rotational Angiography: Recent Experience in the Evaluation of Cerebral Aneurysms for Treatment. Interventional Neuroradiology. 2000;6(2):85-94.

7. Serafin Z, Strześniewski P, Lasek W, Beuth W. Follow-up after embolization of ruptured intracranial aneurysms: A prospective

comparison of two-dimensional digital subtraction angiography, three-dimensional digital subtraction angiography, and time-of-flight magnetic resonance angiography. Neuroradiology. 2012;54(11):1253-1260.

8. Hochmuth A, Spetzger U, Schumacher M. Comparison of Three-Dimensional Rotational Angiography with Digital Subtraction Angiography in the Assessment of Ruptured Cerebral Aneurysms. AJNR. 2002;23:1199-1205.

9. Stapf C, Mast H, Siacca RR, etal. Predictors of hemorrhage in patients with untreated brain arteriovenous malformation. Neurology. 2006;66:1350-1355.

10. J.J.S. Shankar, R.J. Menezes, et al. Angioarchitecture of brain AVM Determines the Presentation with Seizure. AJNR. 2013; 34 (5): 1028-1034.

11. Brown RD Jr, Wiebers DO, Forbes G, et al. The natural history of unruptured intracranial arteriovenous malformations. J Neurosurg. 1988; 68: 352–7.

12. Kaplan HA, Aronson SM, Browder EJ. Vascular malformations of the brain. An Anatomical study. J Neurosurg. 1961; 18: 630-635.

13. Rhoten RLP, Comair YG, Shedid D, Cyatte D, Simonson MS. Specific repression of the preproendothelin-gene in intracranial arteriovenous malformations. J Neurosurg. 1997;86: 101-108.

14. Rothbart D, Awad I, Lee J, et al. Expression of angiogenic factors and structural proteins in central nervous sytem vascular malformations. Neurosurgery. 1996; 38: 915-925.

15. Mullan S, Mojtahedi S, Johnson DL, *etal.* Embryological basis of some aspects of cerebral vascular fistulas and malformations. J Neurosurg. 1996; 85:1–8.

16. Yasargil. Anatomy of the sulci. Microsurgery.1994;Vol IVA: 19

17. Valavanis A. The role of angiography in the evaluation of cerebral vascular malformations. Neuroimaging Clin N Am 1996; 6: 679–704.

18. Valavanis A, Yasargil MG. The endovascular treatment of brain arteriovenous malformations. Advances and Technical Standards in Neurosurgery. 1998;24: 132-182.

19. Yasargil M. AVM of the Brain, History, Embryology, Pathological Considerations, Hemodynamics, Diagnostic Studies, Microsurgical Anatomy. Microneurosurgery New York: Thieme Verlag, 1987.

20. Berenstein A, Lasjaunias P. Surgical Neuroangiography. Berlin, Heidelberg, New York: Springer Verlag, 1991.

21. Russell EJ, Berenstein A. Meningeal collateralization to normal cerebral vessels associated with intracerebral arteriovenous malformations: A functional angiographic study. Radiology. 1991;139:617-622.

22. Faria MA, Fleischer AS. Dural cerebral and meningeal supply to giant arteriovenous malformations of the posterior cerebral hemisphere. J Neurosurg. 1980;52: 153-161.

23. Willinsky RA, Fitzgerald M, TerBrugge K, et al. Brain arteriovenous malformations:Analysis of the angio-architecture in

relationship to hemorrhage. J Neuroradiol. 1988;15: 225-237.

24. Perret G, Nishioka H. Report on the cooperative study of intracranial aneurysms and subarachnoid hemorrhage. Section VI. Arteriovenous malformations. An analysis of 545 cases of cranio-cerebral arteriovenous malformations and fistulae reported to the cooperative study. J Neuro- surg 1966; 25: 467–90.

25. Thompson RC, Steinberg GK, Levy RP, et al. The manage- ment of patients with arteriovenous malformations and associated intracranial aneurysms. Neurosurgery 1998; 43: 202–11.

26. Brown RD Jr, Wiebers DO, Forbes GS. Unruptured intracranial aneurysms and arteriovenous malformations: frequency of intracranial hemorrhage and relationship of lesions. J Neurosurg 1990; 73: 859–63.

27. Turjman F, Massoud TF, Vinuela F, et al. Aneurysms related to cerebral arteriovenous malformations: superselective angiographic assessment in 58 patients. AJNR Am J Neuroradiol 1994; 15: 1601–5.

28. Meisel HJ, Mansmann U, Alvarez H, et al. Cerebral arteriovenous malformations and associated aneurysms: analysis of 305 cases from a series of 662 patients. Neurosurgery 2000; 46: 793–800.

29. Halim AX, Singh V, Johnston SC, et al. Characteristics of brain arteriovenous malformations with coexisting aneurysms: a comparison of two referral centers. Stroke 2002; 33: 675–9.

30. Redekop G, TerBrugge K, Montanera W, et al. Arterial aneurysms associated with cerebral arteriovenous malformations: classification, incidence, and risk of hemorrhage. J Neurosurg 1998; 89: 539–46.

31. Cunha e Sa MJ, Stein BM, Solomon RA, et al. The treatment of associated intracranial aneurysms and arteriovenous malformations. J Neurosurg 1992; 77: 853–9.

32. Westphal M, Grzyska U. Clinical significance of pedicle aneurysms on feeding vessels, especially those located in infratentorial arteriovenous malformations. J Neurosurg 2000; 92: 995–1001.

33. Ezura M, Takahashi A, Jokura H, et al. Endovascular treatment of aneurysms associated with cerebral arterio- venous malformations: experiences after the introduction of Guglielmi detachable coils. J Clin Neurosci 2000; 1: 14–18.

34. Piotin M, Ross IB, Weill A, et al. Intracranial arterial aneurysms associated with arteriovenous malformations: endovascular treatment [see comment]. Radiology 2001; 220: 506–13.

35. Stapf C, Mohr JP, Pile-Spellman J, et al. Concurrent arte- rial aneurysms in brain arteriovenous malformations with haemorrhagic presentation. J Neurol Neurosurg Psychia- try 2002; 73: 294–8.

36. Rinkel GJ, Djibuti M, Algra A, et al. Prevalence and risk of rupture of intracranial aneurysms: a systematic review. Stroke 1998; 29: 251–6.

37. Perata HJ, Tomsick TA, Tew JM Jr. Feeding artery pedicle aneurysms: association with parenchymal hemorrhage and arteriovenous malformation in the brain. J Neurosurg 1994; 80: 631–4.

38. Graf CJ, Perret GE, Torner JC. Bleeding from cerebral arteriovenous malformations as part of their natural history. J Neurosurg 1983; 58: 331–7.

39. Shenkar R, Elliott JP, Diener K, et al. Differential gene expression in human cerebrovascular malformations. Neu- rosurgery 2003; 52: 465–77.

40. McKissock W, Paterson JH. A clinical survey of intracranial angiomas with special reference to their mode of progression and surgical treatment: a report of 110 cases. Brain 1956; 79: 233–66.

41. Inci S, Spetzler RF. Intracranial aneurysms and arterial hypertension: a review and hypothesis. Surg Neurol 2000; 53: 530–40; discussion 40-2.

42. Kerber CW, Liepsch D. Flow dynamics for radiologists. II. Practical considerations in the live human. AJNR Am J Neuroradiol 1994; 15: 1076–86.

43. Kerber CW, Liepsch D. Flow dynamics for radiologists. I. Basic principles of fluid flow. AJNR Am J Neuroradiol 1994; 15: 1065–75.

44. Okamoto S, Handa H, Hashimoto N. Location of intracra- nial aneurysms associated with cerebral arteriovenous malformation: statistical analysis. Surg Neurol 1984; 22: 335–40.

45. Marks MP, Lane B, Steinberg GK, et al. Intranidal aneur- ysms in cerebral arteriovenous malformations: evaluation and endovascular treatment. Radiology 1992; 183: 355–60.

46. Kaptain GJ, Lanzino G, Do HM, et al. Posterior inferior cerebellar artery aneurysms associated with posterior fossa arteriovenous malformation: report of five cases and literature review [see comment]. Surg Neurol 1999; 51: 146–52.

47. Khaw AV, Mohr JP, Sciacca RR, et al. Association of infra- tentorial brain arteriovenous malformations with hemor- rhage at initial presentation. Stroke 2004; 35: 660–3.

48. Kader A, Goodrich JT, Sonstein WJ, et al. Recurrent cere- bral arteriovenous malformations after negative postoper- ative angiograms [see comment]. J Neurosurg 1996; 85: 14–18.

49. Mahajan A, Manchandia TC, Gould G, et al. De novo arte- riovenous malformations: case report and review of the literature. Neurosurg Rev 2010; 33: 115–19.

50. Berenstein A, Lasajaunias P, Choi IS. Endovascular treatment of arteriovenous malformations of the brain. Interventional Neuroradiology. 1993; pp 93.

51. Ondra SL, Trouppp H, George ED, Schwab. The natural history of symptomatic arteriovenous malformations of the brain: a 24 year follow up assessment. J Neurosurg. 1990;73: 387-392.

52. Valavanis A. Neuroradiological evaluation: AVM of the brain, history, embryology, pathological considerations, hemodynamics, diagnostic studies, microsurgical anatomy. Microsurgery. 1987;

Vol III A: 250-283.

53. X. Combaz, O. Levrier, J. Moritz, et al. Three-dimensional rotational angiography in the assessment of the angioarchitecture of brain arteriovenous malformations. J Neuroradiol. 2011;38:167-174.

54. Racadio JM, Fricke BL, Jones BV, Donnelly LF. Three-dimensional rotational angiography of neurovascular lesions in pediatric patients. AJR 2006;186(1):75-84.

55. Schueler BA, Kallmes DF, Cloft HJ. 3D cerebral angiography: radiation dose comparison with digital subtraction angiogra- phy. AJNR 2005;26(8):1898—901.

56. Gosch D, Kurze W, Deckert F, Schulz T, Patz A, Kahn T. Radiation exposure with 3D rotational angiography of the skull. Rofo 2006;178(9):880—5.

57. Kawashima M, Kitahara T, Soma K, Fujii K. Three-dimensional digital subtraction angiography vs two-dimensional digital subtraction angiography for detection of ruptured intracranial aneurysms: a study of 86 aneurysms. Neurology India. 2005;53: 287-289.

58. Takeshi Sugahara, Yukunori Korogi, Kouji Nakashima, et al. Comparison of 2D and 3D Digital Subtraction Angiography in Evaluation of Intracranial Aneurysms. Am J Neuroradiol. 2002;23: 1545–1552

59. Hasegawa H, Hanakita S, Masahiro Shin, *et al*. Integration of rotational angiography enables better dose planning in Gamma

Knife Radiosurgery for brain arteriovenous malformations. J Neurosurg. 2018;129: 17-25.

60. Raphaël Blanc, Aude Seiler, Thomas Robert, et al. Multimodal angiographic assessment of cerebral arteriovenous malformations: a pilot study. J NeuroIntervent Surg 2015;7: 841–847.

61. Fiorella D, Albuquerque FC, Woo HH, McDougall CG, Rasmussen PA. The role of neuroendovascular therapy for the treatment of brain arteriovenous malformations. Neurosurgery 2006;59 (5 Suppl 3): S163—77

62. Turjman F, Massoud TF, Vinuela F, Sayre JW, Guglielmi G, Duckwiler G. Correlation of the angioarchitectural features of cerebral arteriovenous malformations with clinical presentation of hemorrhage. Neurosurgery 1995;37(5):856-60.

63. Michael J Ellis, Derek Armstrong, Shobhan Vachhrajani, et al. Angioarchitectural features associated with hemorrhagic presentation in pediatric cerebral arteriovenous malformations. J NeuroIntervent Surg 2013;5:191–195.

64. Crawford PM, West CR, Chadwick DW, Shaw MD. Arteriovenous malformationsof brain: natural history in unoperated patients. J Neurol Neurosurg Psychiatry. 1986;49: 1-10.

65. Shankar JJS, Menezes RJ, Pohlman EB, et al. Angioarchitecture of Brain AVM Determines the Presentation with Seizures: Proposed Scoring System. Am J Neuroradiol . 2013;34: 1028 –34.

66. Dale Ding, Robert M. Starke, Mark Quigg, Chun-Po Yen, Colin J. Przybylowski, Blair K. Dodson, Jason P. Sheehan. Cerebral

Arteriovenous Malformations and Epilepsy, Part 1: Predictors of Seizure Presentation. World Neurosurgery. 2015; 84 [3]: 645-652.

67. Ellis JA, Mejia Munne JC, Lavine SD, et al. Arteriovenous malformations and headache. J Clin Neurosci. 2016;23: 38-43.

68. Spetzler RF, Hargraves RW, McCormick PW, et al. Relationship of perfusion pressure and size to risk of haemorrhage from arteriovenous malformations. J Neurosurg. 1992; 76: 918-923.

69. Pollock BE, Flickinger JC, Lunsford LD, Bissonette DJ, Kondziolka D. Factors that predict the bleeding risk of cerebral arteriovenous malformations. Stroke.1996;27:1–6.

70. Stefani AM, Porter PJ, et al., Angioarchitectural Factors Present in Brain Arteriovenous Malformations Associated With Hemorrhagic Presentation. Stroke. 2002;33:920-924.

71. Rammos SK, Gardenghi B, Bortolotti C, *et al*. Aneurysms associated with brain arterivenous malformations. Am J Neuroradiol. 2016;37: 1966 –71

72. Mjaoli N, Feuvre D, Taylor A. Bleeding source identification and treatment in brain arteriovenous malformations. Interventional Neuroradiology. 2011;17: 323-330.

73. Francis Turjman, Tarik F. Massoud, James W. Sayre, Fernando Vinuela, Guido Guglielmi, and Gary Duckwiler. Epilepsy associated with cerebral arteriovenous malformations: a multivariate analysis of angioarchitectural characteristics. AJNR. 1995;16: 345–350.

ANNEXURES

APPENDIX A

श्री चित्रा तिरुनाल आयुर्विज्ञान और प्रौद्योगिकी संस्थान, त्रिवेन्द्रम
तिरुवनन्तपुरम - ६९५०११, केरल, इंडिया
SREE CHITRA TIRUNAL INSTITUTE FOR MEDICAL SCIENCES AND TECHNOLOGY, TRIVANDRUM
Thiruvananthapuram - 695 011, Kerala, India
(An Institute of National Importance under Govt. of India)
Grams : Chitramet, Phone : +91-471-2443152, Fax : +91-471-2550728 / 2446433, E-mail : sct@sctimst.ac.in, Website : www.sctimst.ac.in

Institutional Ethics Committee
(IEC Regn No. ECR/189/Inst/KL/2013)

SCT/IEC/1088/AUGUST-2017 07.10.2017

Dr. Somnath Pan
Senior Resident
Department of IS & IR
SCTIMST, Thiruvananthapuram

Dear Dr. Somnath Pan,

The Institutional Ethics Committee reviewed and discussed your application to conduct the study entitled "COMPARISON OF 3D ROTATIONAL ANGIOGRAPHY WITH DIGITAL SUBTRACTION ANGIOGRAPHY AND CORRELATION OF ANGIOARCHITECTURE WITH CLINICAL PRESENTATIONS IN CEREBRAL ARTERIOVENOUS MALFORMATIONS (IEC/1088)" on 19th August, 2017.

The following documents were reviewed:

Original submission

1. Covering letter addressed to the Chairperson, IEC, SCTIMST dated 13.07.2017 with checklist
2. TAC Approval Letter
3. IEC Application Form
4. Project Proposal
5. Informed Consent Form in English and Malayalam
6. Proforma
7. CV of Principal Investigator and Co-Principal Investigators

Revised submission

1. Covering letter addressed to the Chairperson, IEC, SCTIMST dated 22.09.2017 with checklist
2. TAC Approval Letter
3. IEC Application Form
4. Project Proposal
5. Informed Consent Form in English and Malayalam
6. Proforma
7. CV of Principal Investigator and Co-Principal Investigators

The following members of the Ethics Committee were present at the meeting held on 19th August, 2017 at G. Parthasarathi Board Room, AMCHSS, SCTIMST

SL No	Member Name	Highest Degree	Gender	Scientific /Non Scientific	Affiliation with Institution(s)
1.	Dr. R V G Menon	M Tech, PhD	Male	Lay Person (Chairman)	No
2.	Dr.Lekha Pandit	MD.DM Neurology, PhD (Bioscience)	Female	Clinician	No
3.	Dr. Kala Kesavan. P	MBBS, MD	Female	Basic Medical Scientist	No
4.	Dr. Rema M. N	MD	Female	Basic Medical Scientist	No
5.	Dr. S S Giri Sankar	LL.M. Ph.D.	Male	Legal Expert	No
6.	Dr. Aneesh V Pillai	BA. LLB (Hons.), LLM, Ph. D, SET (Law)	Male	Legal Expert	No
7.	Mr. Satheesh Chandran	MSW, PGDPM	Male	Lay person/ NGO/ Social Scientist	No
8.	Smt. Sathi Nair	MA (English Literature)	Female	Lay Person	No
9.	Dr. P. Manickam	BSMS, MSc (Epid).,PhD	Male	Health Science Expert/ Social Scientist	No
10.	Dr. Christina George	MD Psychiatry	Female	Clinician	No
11.	Dr. V. Raman Kutty	M D, M Phil, M P H	Male	Health Sciences Expert/Clinician	Yes
12.	Dr. K R S Krishnan	M.E., Ph.D.	Male	Medical Technology	Yes
13.	Dr. Harikrishna Varma PR	Ph.D(Materials Science)	Male	Medical Technology	Yes
14	Dr. Harikrishnan S	MD, DM (Cardiology) DNB (Cardiology)	Male	Clinician	Yes
15.	Dr. Mala Ramanathan	PhD	Female	Social Scientist (Member Secretary)	Yes

IEC Decision

The IEC approved the conduct of the study in the present form.

Remarks:
The Institutional Ethics Committee expects to be informed about the progress of the study, any SAE occurring in the course of the study, any changes in the protocol and patient information/informed consent and asks to be provided a copy of the final report.

There was no member of the study team who participated in voting / decision making process. The ethics committee is organized and operated according to the requirements of Good Clinical Practice and the requirements of the Indian Council of Medical Research (ICMR).

Sincerely,

Mala Ramanathan
Member Secretary, IEC

APPENDIX B

INFORMATION SHEET

TITLE OF THE STUDY: COMPARISON OF 3D ROTATIONAL ANGIOGRAPHY WITH DIGITAL SUBSTRACTION ANGIOGRAPHY AND CORRELATION OF ANGIOARCHITECTURE WITH CLINICAL PRESENTATIONS IN CEREBRAL ARTERIOVENOUS MALFORMATIONS

Study number:

Participant's name: Date of Birth / Age (in years): son/daughter of _____

You have been informed that there is an abnormal communication between the arteries and veins within your brain parenchyma, (which is called Arteriovenous malformation), for which, you have undergone or will be undergoing a digital subtraction angiography (DSA) test as a part of clinical evaluation of your disease to plan the treatment or for follow up your disease.

The brain arteriovenous malformation is a disease of blood vessels in the brain where the blood vessels remain entangled in certain locations of the brain, thought to exist since birth. The blood is shunted across these communications at a rapid pace and changes occur within or adjacent to this region is responsible for the development of clinical symptoms. Symptoms are variable and may be correlated or predicted with angiographic appearance in certain situations.

You are being requested to participate in a study to evaluate the role of 3D rotational angiography in assessment of arteriovenous malformations

and to analyse possible angiographic predictors for clinical manifestations like haemorrhage, seizure & neurodeficts. Participating in this study, in which only data from the investigations you have undergone for your treatment will be used, will in no way influence treatment decisions.

What is DSA/3D rotational angiography and does it have any harmful effects?

DSA is an advanced imaging technique where the blood flow to your brain will be evaluated by injecting a dye into the arteries to the brain through a small tube which will be inserted through the artery in your groin. X Rays will be obtained during the procedure which will clearly show the abnormal connections between arteries and veins if they exist. 3D rotational angiography is an advanced technique in DSA in which images are obtained during rotation of the X-ray tube head. You will not experience much pain as an injection will be given on your groin prior to the procedure to make it numb. You will not feel any pain during the rest of the procedure. In rare cases some people may have allergic reaction to the dye. There is also a very small risk of injury to the blood vessel and slight chance of bleeding at site of puncture. This test is vital in diagnosis of your condition and is also the means of treatment if planned subsequently.

If you take part what will you have to do?

- For this study, we'll be using some of the data like history and other clinical details, Imaging details (CT/MRI/ CTA /MRA), Angiograms (DSA), treatment technique, outcome of the procedure, delayed follow up clinical and radiological regarding your disease and treatment which you undergo in this hospital.

 No additional cost will be incurred /no additional drugs will be used and there are no additional risks as a part of the research.

 Analysis of these data may or may not be useful for you later, but this is likely to give more understanding of this disease and treatment, for the benefit of future generation. You understand that strict confidentiality will be maintained.

Can you withdraw from this study after it starts?

Your participation in this study is entirely voluntary and you are also free to decide to withdraw permission to participate in this study. If you do so, this will not affect your usual treatment at this hospital in any way.

What will happen if you develop any study related injury?

This study only analyzes the results of your investigation and treatment details and thus we do not expect any injury to happen to you but if you do develop any side effects or problems due to the study, these will be treated at this institute by the experienced team of medical professionals. We are unable to provide any monetary compensation, however.

Will you have to pay for the study?

The study will only analyze the results of the investigations and treatment which you will undergo in natural process of your treatment at this institute and no extra cost will be borne by you for this particular study.

What happens after the study is over?

You may or may not benefit from this study, after the study we will be able to assess the utility of 3D rotational angiography & angiographic predictors for clinical manifestations; it may thus benefit other patients

with similar illness.

Will your personal details be kept confidential?

The results of this study may be published in a medical journal but you will not be identified by name in any publication or presentation of results. However, your medical notes may be reviewed by people associated with the study, without your additional permission, should you decide to participate in this study.

If you have any further questions, please ask Dr. Somnath Pan (tel: 8768874707) or email: snpan96@sctimst.ac.in or contact IEC member secretary (tel: 0471-2524263)

APPENDIX C

CONSENT FORM

TITLE OF THE STUDY: COMPARISON OF 3D ROTATIONAL ANGIOGRAPHY WITH DIGITAL SUBSTRACTION ANGIOGRAPHY AND CORRELATION OF ANGIOARCHITECTURE WITH CLINICAL PRESENTATIONS IN CEREBRAL ARTERIOVENOUS MALFORMATIONS

Study number:

Participant's name: Date of Birth / Age (in years):
I_____
_____Son/daughter of _____
(Please tick boxes)

• Declare that I have read the above information provide to me regarding the study: 'Comparison of 3D rotational angiography with digital subtraction angiography and correlation of angioarchitecture with clinical presentations in cerebral arteriovenous malformations' and have clarified any doubts that I had. [ ]

• I also understand that my participation in this study is entirely voluntary and that I am free to withdraw permission to continue to participate at any time without affecting my usual treatment or my legal rights. [ ]

• I also understand that study investigators will be using some of the data like history and other clinical details, Imaging details (CT/MRI/ CTA /MRA), Angiograms (DSA), Embolisation technique, outcome of the procedure(Immediate angiographic and clinical) , delayed follow up clinical and radiological regarding the disease and treatment which I

undergo in hospital. [ ]

• I also understand that no additional cost will be incurred /no additional drugs will be used and there are no additional risks as a part of the research. [ ]

• I understand that the study staff and institutional ethics committee members will not need my permission to look at my health records even if I withdraw from the trial. I agree to this access. [ ]

• I understand that my identity will not be revealed in any information released to third parties or published. [ ]

• I voluntarily agree to take part in this study. [ ] • I received a copy of this signed consent form. [ ] Name: Signature: Date: Name of witness: Relation to participant:

Date:

(Person Obtaining Consent) I attest that the requirements for informed consent for the medical research project described in this form have been satisfied. I have discussed the research project with the participant and explained to him or her in nontechnical terms all of the information contained in this informed consent form, including any risks and adverse reactions that may reasonably be expected to occur. I further certify that I encouraged the participant to ask questions and that all questions asked were answered.

_____	_____
Name and Signature of Person Obtaining Consent	Principal Investigator.

APPENDIX D

PROFORMA

Title: COMPARISON OF 3D ROTATIONAL ANGIOGRAPHY WITH DIGITAL SUBSTRACTION ANGIOGRAPHY AND CORRELATION OF ANGIOARCHITECTURE WITH CLINICAL PRESENTATIONS IN CEREBRAL ARTERIOVENOUS MALFORMATIONS

Anonymized patient key :
CLINICAL:
Age:
Sex:
Chief complaints/duration of symptoms:
History of presenting complaints: Symptoms suggestive of acute intracranial haemorrhage: Seizure : Headache: Neurodeficit :
Past history/treatment history:
Examination :
General examination:

System examination:
CVS

Respiratory

GIT/GUT

CNS:

Higher mental function

Speech

Cranial nerve

Motor system

Sensory system

Cerebellar assessment

Tandem Gait

Other /Local examination:

IMAGING REVIEW

CT/MRI :

Location of lesion –

Haemorrhage –

Others

2D DSA

➢ Image identification number:	
➢ Investigator:	
➢ Study : DSA	
➢ Date of Image analysis:	
➢ Quality of image: assess considering	
1. overall quality of distal vessel identification,	
2. Visualisation of the nidus.	
➢ five-point scale score:	
▪ 4 excellent quality;	
▪ 3, adequate quality for diagnosis;	
▪ 2, less than adequate quality for diagnosis;	
▪ 1, nondiagnostic.	
➢ Findings:	
1. Lesion side : Right / Left / Midline	
2. BAVM size (mm).....(CC x TR AP)	
3. BAVM border with adjacent brain (on DSA)	
1. Compact (sharp)	
2. Diffuse	
Sparse	
3. Periventricular drainage (yes/no)	
4. Number of draining veins leaving nidus (count)	
5. Number of veins reaching sinus (count)	

6. Venous stenosis/occlusion (number; percentage, where 100% occlusion)	
7. Venous ectasia (dilatation) (yes/no)	
8. Venous reflux (yes/no)	
9. Sinus thrombosis/occlusion (number; percentage, where 100% occlusion)	
4. Arterial supply	
1. Feeding arteries : Choose all applicable:	
i. Anterior choroidal a.	
ii. Posterior choroidal a.	
iii. Anterior cerebral a. cortical branches	
iv. Anterior cerebral a. penetrators	
v. Middle cerebral a. cortical branches	
vi. Middle cerebral a. penetrators	
vii. Posterior cerebral a. cortical branches	
viii. Posterior cerebral a. penetrators	
ix. Superior cerebellar a.	
x. Anterior inferior cerebellar a.	
xi. Posterior inferior cerebellar a.	
xii. Basilar a. penetrators	
xiii. Vertebral a. penetrators	
xiv. Vertebral a. branches	
xv. Internal carotid a. penetrators	
xvi. Other internal carotid a. branches	
xvii. External carotid a. branches	

xviii. Other a.	
2. Arterial aneurysms	
i. Number of arterial aneurysms (count)	
ii. Arterial aneurysms location Pick all applicable to any aneurysm:	
1. Flow-related	
2. Proximal	
3. Not flow-related	
4. Distal	
5. Nidal	
iii. Arterial aneurysms hemorrhagic history (yes/no)	
iv. Arterial aneurysms hemorrhagic (date)	
v. Number of vessels to be embolized (count)	
vi. Moyamoya-type changes (yes/no)	
vii. Pial-to-pial collateralization : Choose all applicable	
1. Same territory	
2. Between territories	
3. None	

3D RA

➢ Image identification number:	
➢ Investigator:	
➢ Study : 3D RA	
➢ Date of Image analysis:	
➢ Quality of image: assess considering	
1. overall quality of distal vessel identification,	
2. Visualisation of the nidus.	
➢ five-point scale score:	
▪ 4 excellent quality;	
▪ 3, adequate quality for diagnosis;	
▪ 2, less than adequate quality for diagnosis;	
▪ 1, nondiagnostic.	
➢ Findings:	
1. Lesion side : Right / Left / Midline	
5. BAVM size (mm).....(CC x TR AP)	
6. BAVM border with adjacent brain (on DSA)	
1. Compact (sharp)	
2. Diffuse	
7. BAVM hemorrhage	
1. Evidence of NEW BAVM hemorrhage (yes/no)	
2. Age of NEW BAVM hemorrhage (integer; day)	
3. Is NEW BAVM hemorrhage symptomatic? (yes/no)	
4. Evidence of OLD BAVM hemorrhage (yes/no)	
5. Age of OLD BAVM hemorrhage (integer; mo)	
6. Was OLD BAVM hemorrhage symptomatic? (yes/no)	
7. Hemorrhage location : Choose all applicable:	
i. Ventricular	
ii. Parenchymal	
iii. Subarachnoid	
8. Hemorrhage size (mm) …….(CC x TR x AP)	
8. Venous drainage	
1. Superficial vs deep venous drainage	
i. Both superficial and deep	

ii. Superficial only	
iii. Deep only	
2. Periventricular drainage (yes/no)	
3. Number of draining veins leaving nidus (count)	
4. Number of veins reaching sinus (count)	
5. Venous stenosis/occlusion (number; percentage, where 100% occlusion)	
6. Venous ectasia (dilatation) (yes/no)	
7. Venous reflux (yes/no)	
8. Sinus thrombosis/occlusion (number; percentage, where 100% occlusion)	
9. Arterial supply	
1. Feeding arteries : Choose all applicable:	
i. Anterior choroidal a.	
ii. Posterior choroidal a.	
iii. Anterior cerebral a. cortical branches	
iv. Anterior cerebral a. penetrators	
v. Middle cerebral a. cortical branches	
vi. Middle cerebral a. penetrators	
vii. Posterior cerebral a. cortical branches	
viii. Posterior cerebral a. penetrators	
ix. Superior cerebellar a.	
x. Anterior inferior cerebellar a.	
xi. Posterior inferior cerebellar a.	
xii. Basilar a. penetrators	
xiii. Vertebral a. penetrators	
xiv. Vertebral a. branches	
xv. Internal carotid a. penetrators	
xvi. Other internal carotid a. branches	
xvii. External carotid a. branches	
xviii. Other a.	
2. Arterial aneurysms	
i. Number of arterial aneurysms (count)	
ii. Arterial aneurysms location Pick all applicable to any aneurysm:	
1. Flow-related	
2. Proximal	
3. Distal	

4. Nidal	
iii. Arterial aneurysms hemorrhagic history (yes/no)	
iv. Arterial aneurysms hemorrhagic (date)	
v. Moyamoya-type changes (yes/no)	
vi. Pial-to-pial collateralization : Choose all applicable	
1. Same territory	
2. Between territories	
3. None	

Spetzler Martin grade:

Plagiarism Checker by Grammarly

Grammarly's plagiarism checker detects plagiarism in your text and checks for other writing issues.

Nidus appearance: Three types of appearance of the nidus were determined independently by evaluating the DSA and 3D RA images.
a) Compact nidus: Close-packed arteriovenous shunting zone (nidus) with well defined borders and homogeneous appearance (as there is no intervening normal brain tissue).
b) Diffuse nidus: Diffuse appearance of the nidus involving a large lobar or

Scan for plagiarism Upload a file

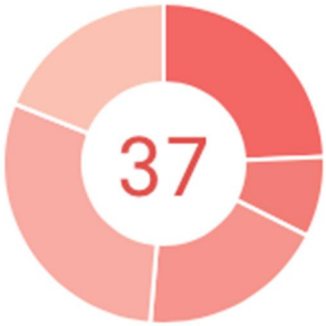

Plagiarism was not detected

We didn't find any plagiarism, but we found 37 writing issues.

KEY TO MASTER CHART

Y	-	Yes
N	-	No
C	-	Compact
D	-	Diffuse
S	-	Sparse
FND	-	Neurological symptoms and deficits
PN	-	Perinidal
FA	-	Feeding Artery